March 2010

UTILIZING LEDs AS FEEDBACK SENSORS FOR VIDEO DISPLAYS

Daniel Paul Cianfrocco
Worcester Polytechnic Institute

Eric Joseph Renzulli
Worcester Polytechnic Institute

Tuen Hung Lee
Worcester Polytechnic Institute

Project Number: MQP-SJB-1A09

UTILIZING LEDs AS FEEDBACK SENSORS FOR VIDEO DISPLAYS

A Major Qualifying Project Report

Submitted to the Faculty

of

WORCESTER POLYTECHNIC INSTITUTE

In partial fulfillment of the requirements for the

Degree of Bachelor of Science

in

Electrical and Computer Engineering

by

_____

Dan Cianfrocco

_____

Tuen Hung Lee

_____

Eric Renzulli

March 5, 2010

Sponsoring Organization:
NECAMSID

_____

Professor Stephen J. Bitar, Major Advisor

_____

Professor John A. McNeill, Co-Advisor

Abstract

The purpose of this project was to demonstrate as a proof of concept that LED emitters within outdoor video displays can also be utilized as optical feedback sensors for self-calibration. The emission and sensing characteristics of new and degraded LEDs were measured and studied to determine the effectiveness of using LEDs as sensors. A small-scale, adjustable LED driver with a closed-loop feedback control system was designed to illustrate self-calibration without extra sensing components. LED current was automatically adjusted to maintain proper LED brightness and color, while utilizing an adjacent LED as a sensor. Test results show that the self-calibration control system is viable and effective. Further work is necessary to determine system proficiency for large scale LED video displays.

Executive Summary

LEDs have been universally used in many applications as light emitters in recent years due to rapid technological advancements. They are widely known for their energy efficiency, low heat dissipation, small size, durability, and long lifetime. One of the applications that LEDs have dominated is large-scale outdoor video displays, such as stadium displays, billboards, and large outdoor televisions. Before LEDs, projection was the only large-scale method for video displays. LEDs have allowed screens to become much thinner and modular, while also greatly improving light output and viewing angles. However, one major problem still present is the unpredictable degradation of LEDs resulting in color inaccuracy and differences in brightness among neighboring emitters. Though LEDs are billed by the industry as long lasting, studies have shown that LED output can vary by as much as 40% in their first 500 hours of use (Grillot, et al. 2006). Currently, calibrating an LED display requires either sending it to the factory or having a technician come on site with extensive equipment; both of which are very costly and inefficient. The purpose of this project was to eliminate this problem by demonstrating as a proof of concept that LEDs can be used as both a light emitter as well as an optical feedback mechanism in outdoor video display applications. Using feedback, a control system within the display driver can calibrate the display itself to improve color and brightness output quality. However, we decided that building an actual LED display would not be feasible within the time constraint of this project. Therefore, we designed a small-scale adjustable LED driver with a closed-loop feedback control system that uses LEDs as both emitters and sensors.

To realize this system, we took advantage of the p-n junction within the LED. As an emitter, the p-n junction is forward-biased, allowing the current to flow through the junction to produce light. By controlling both the level and duty cycle of the current, brightness and color spectrum of the light output can be varied. As a light sensor, the p-n junction is reverse-biased, stopping current from flowing past the junction. However, when enough light from a nearby source, such as another LED of similar wavelength, hits the depletion region, the electric field in the depletion region will accelerate the electrons towards the N-layer and the holes towards the P-layer. This action results in the LED creating a current proportional to the incident light striking the diode. This current is measured using a novel method requiring only two digital logic pins and no extra

components. Interpreting this current through a feedback control system enables closed loop operation.

There were two main stages of the design and implementation aspect of our project. The first phase was LED characterization. We tested new and degraded red, blue, and green discrete oval LEDs from four manufacturers using a Red Tide Spectrometer. The LEDs were degraded by stressing them with a high DC current. The emission spectrum and intensity of the degraded LEDs were compared to those of the new LEDs, to determine how the degradation affected the LEDs' ability to emit and sense light. The second phase of our design was implementing the test system. We designed a system utilizing a Field-Programmable Gate Array (FPGA) to control the user inputs for current and PWM and also to control and manipulate the feedback from the LED sensor. One LED was used as an emitter and another as a sensor. Both LEDs were connected to the driver circuit, and toggled in an alternating fashion. So while one LED was emitting light, the other LED was connected to an FPGA and acted as a sensor.

The results we got for the first stage were very pleasing. LEDs were degraded to approximately 50% brightness in batches of blue, red, and green by driving them with 50mA and 100mA of current for an extended period of time. Then, we characterized the spectrums of the new and degraded LEDs using the USB650 Red Tide Spectrometer. The data showed that there was very little color shift, with most of the differences falling within 3 nanometers. We concluded that the degradation did not hamper the LED's ability to detect another LED of the same color. For the second stage, the prototype system functioned as we desired. In emission mode, it was capable of driving two LEDs at a desired current level, frequency, and duty cycle. In sensing mode, the detecting LED was effective in measuring the brightness of other LEDs of the same color. In addition, the feedback control loop was able to calibrate the emitting LED using data provided by the LED sensor.

The results of this project demonstrated concrete support that LEDs can be used as emitters as well as optical feedback sensors. We are very pleased with the outcome and see potential for this technique. Improvements such as a more symmetrical LED driver, a more accurate degradation

process, and optimizations would constitute further work for this project. Implementing this concept on a large scale (LED panel) would also be a great step forward.

Acknowledgments

We would like to thank the following individuals and organizations for their support of our project. This project would not have been possible without Professor McNeill and the sponsors of the New England Center for Analog and Mixed Signal Integrated Circuit Design (NECAMSID). We would also like to thank Professor Quimby and the WPI IPG Photonics Lab for letting us use their optical test equipment. Professor Jarvis also helped us develop software for our FPGA. We would like to thank Avago Technologies, Cree, and Nichia Corporation for providing LED test samples. And finally, we would like to thank our advisor, Professor Bitar, for asking the right questions at the right times.

Table of Contents

Table of Figures

Table of Tables

1. Background Research

The first step in our project was to gather general information on LEDs.

1.1. LED Basics

LEDs are a special type of diode that can emit light, and have been used for many different applications throughout their lifetime. Initially, they could only be used as indicators, as the first LEDs only could produce red colors with a low intensity. After other colors became widely available, LEDs emerged as the clear choice for indication and status illumination due to their low power dissipation. LED technology has grown to allow manufacturers to develop better discrete and high-intensity LEDs that are also very efficient. The newer and brighter LEDs have expanded the possible applications for LEDs, including traffic lights and video displays. Most recently, white LEDs have been developed for use in lighting applications.

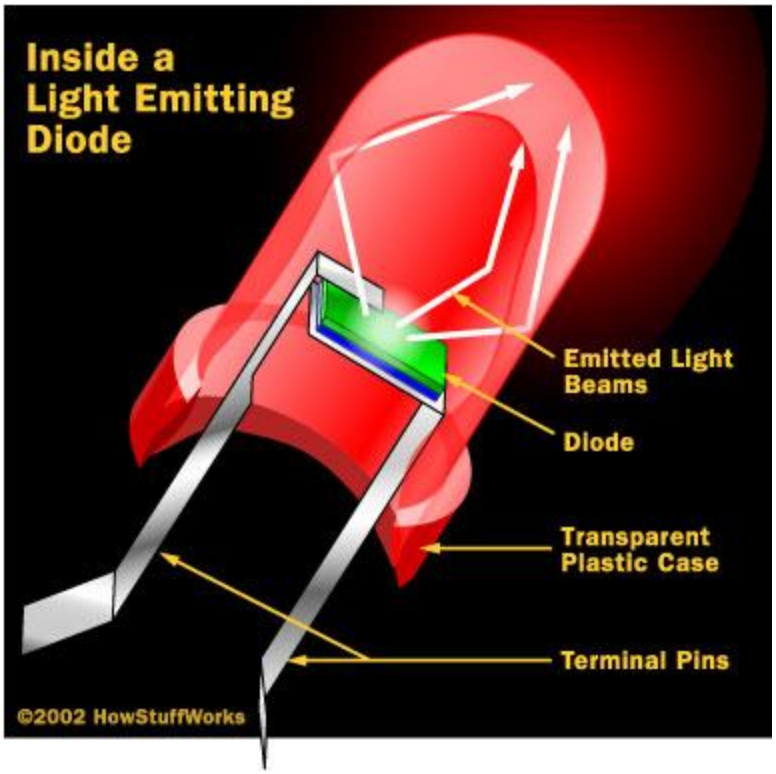

Figure 1: Inside a LED(Harris T. , 2002)

An LED is similar to a normal diode, and contains semiconductor material that is doped to create a p-n junction. A p-n junction consists of three major regions. The first two regions are p-type conductive material and n-type conductive material, where the conductive material is usually silicon. P-type silicon is created by doping the material with an element that will remove weakly bonded electrons to create electron holes. N-type silicon is created by doping the material with an element that will donate electrons to increase the total number of free electrons. When these two regions are joined together, the extra electrons in the n-type region fill the extra electron holes from the p-type material at the junction between the two layers. This creates the third region called the depletion region. This region is not conductive, and does not allow current to flow. A p-n junction can be seen in Figure 2.

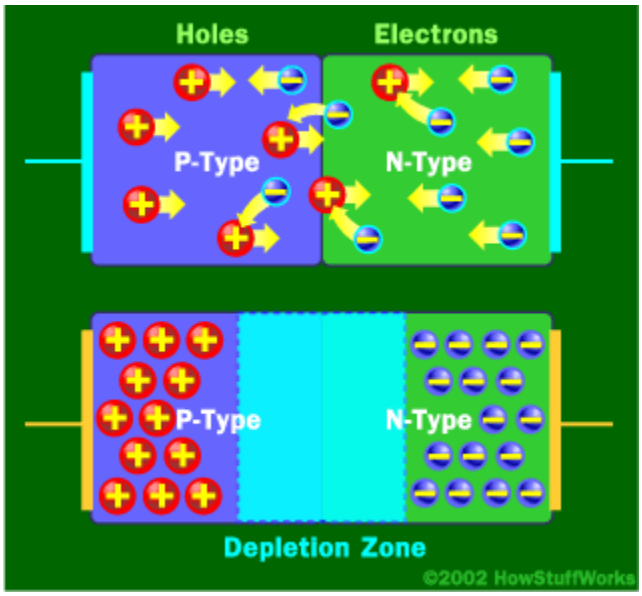

Figure 2: P-N Junction(Harris S. , 2009)

However, when the p-n junction is forward-biased, meaning the p-type region is connected to a positive supply and the n-type region is connected to a negative supply, current can flow through the junction. When a voltage is applied, the holes in the p-type region are repelled from the positive supply and the electrons in the n-type region are repelled from the negative supply. When the forward voltage is high enough, the electrons are removed from the holes in the depletion region, causing current to flow. A forward biased p-n junction can be seen in Figure 3.

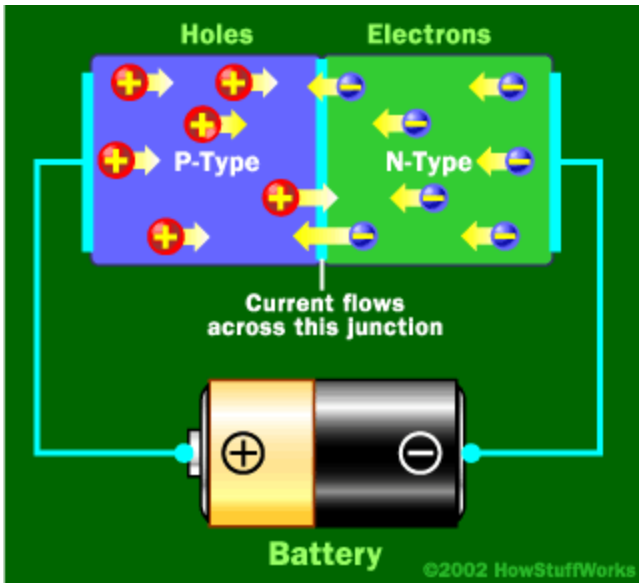

Figure 3: P-N Junction Forward Biased(Harris S. , 2009)

Current will not flow if the p-n junction is reverse-biased, as the holes will be attracted to the negative supply and the electrons will be attracted to the positive supply, which just enlarges the depletion region. A reverse biased p-n junction can be seen in Figure 4.

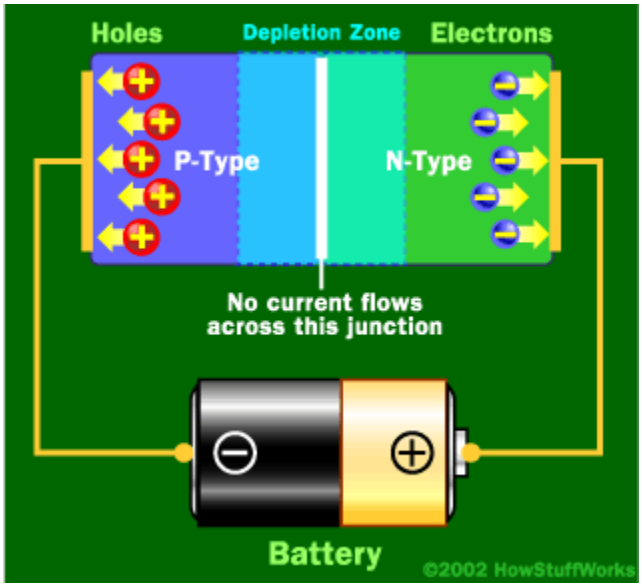

Figure 4: P-N Junction Reverse Biased(Harris S. , 2009)

1.2. LEDs as Emitters

Light is produced when an electron fills a hole and falls to a lower energy level, releasing a photon in the process. A greater energy gap between the two levels releases a higher energy proton, measured in frequency. The color of the light is dependent on the size of the drop between energy levels. Standard silicon diodes are designed to have a small drop between energy levels, so the photons they emit are not visible. To produce visible light, LED manufacturers make the p-n junctions out of materials that have a higher band gap such as gallium-based crystals.

LEDs are very monochromatic, emitting light in a narrow range of frequency. The narrow band of frequency results in limited but distinct color. The color of light emitted by a LED is identified by its peak wavelength, measured in nanometers. For typical human eyes, the visible spectrum ranges from about 380nm to 750nm. Conventional red, green, and blue LEDs have peak wavelength of 625nm, 525nm, and 470nm respectively. All of the colors in the visible spectrum can be produced by using a combination of red, green, and blue LEDs.

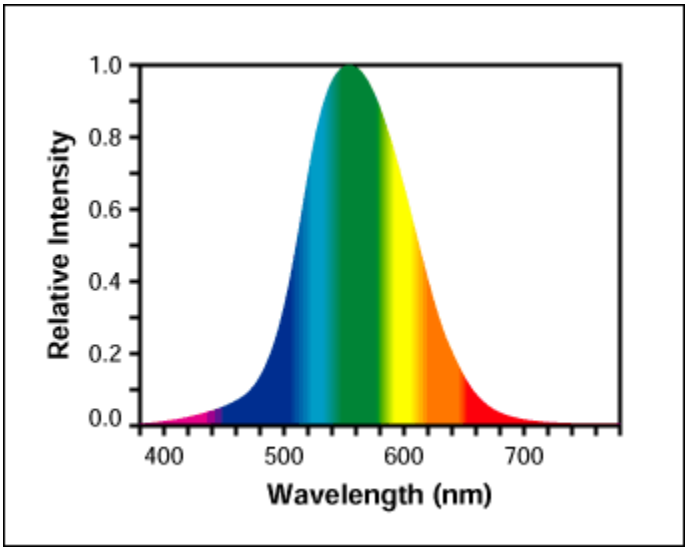

Figure 5: The Visible Spectrum (Maxim, 2003)

The intensity of the light LED produces is measured in millicandela (mcd). Different LEDs can emit tens to tens of thousands millicandela of light. Many manufacturers would characterize LEDs as standard brightness or high brightness according to the luminous intensity, although

there are no industry standards on where to draw the line between the two types of LEDs. The variation of light output level can be a result of the type of chip, encapsulation, efficiency of individual wafer lots and other variables. The intensity is also related to the driving current of the LED. With a higher operating current, the LED can emit in a higher intensity. However, there are design limits on how much current can be inputted to LEDs. Heat dissipation and degradations are the major factors in considering operating current. (The LED Light, 2000)

1.3. LEDs as Detectors

When used as a sensor, LEDs behave identically to PN-based photodiodes. When light is allowed to strike the P-layer, it is dispersed through each layer of the diode. The shortest wavelengths are absorbed by the P-layer, and the longest wavelengths are absorbed by the N-layer. The wavelengths absorbed by the depletion region are controlled by the thickness and doping concentrations of each layer. If the light absorbed in the depletion region is greater than the band gap energy, electrons will jump to the conduction band leaving a hole in the valence band. The electric field in the depletion region then accelerates the electrons towards the N-layer and the holes towards the P-layer. As a result, if a circuit is connected to the leads of the LED, the electrons will flow from the N-layer to the P-layer creating a current proportional to the incident light striking the diode.(Hamamatsu Photonics, K. K., 2008)

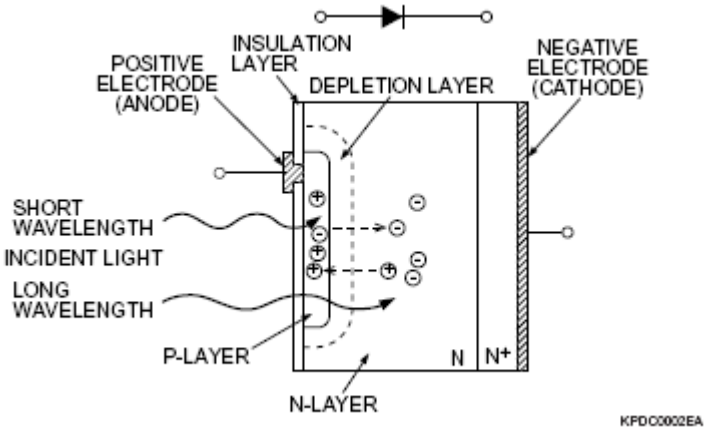

Figure 6: P-N Junction of a LED Operating as a Sensor (Hamamatsu Photonics, K. K. 2008)

A research on LEDs as detectors has shown the LEDs' emission and detection spectrum do not match well with each other. The spectrum shift in green LEDs resulted in very little overlapping of the emission and detection spectrum. This phenomenon is more significant in the blue LEDs, the two spectra do not overlap at all. This may cause problem with the LED's capability of detecting its own emission. (Miyazaki, Itami, & Araki, 1998)

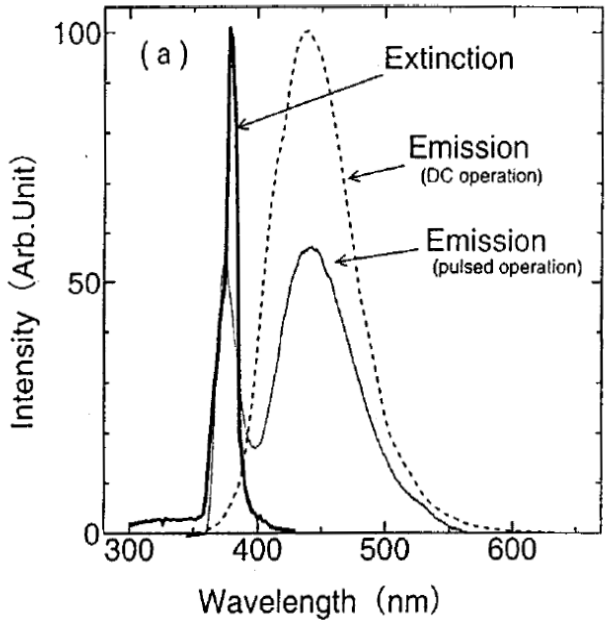

Figure 7: Emission and Detection Spectrum of Blue LED (Miyazaki, Itami, & Araki, 1998)

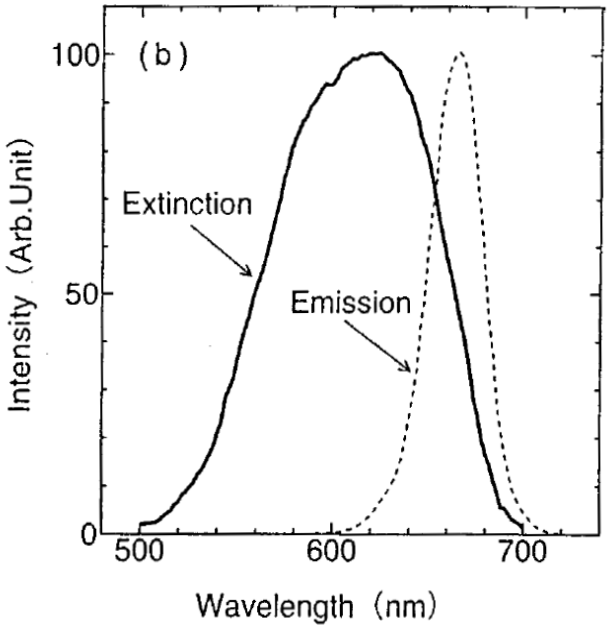

Figure 8: Emission and Detection Spectrum of Green LED (Miyazaki, Itami, & Araki, 1998)

1.4. LED Degradation

Unlike incandescent lamps, LEDs do not have a filament that can break or a gas envelop that can crack. As a result, LEDs do not simply go out at their end of life. Instead, they gradually lose output luminosity over time, as shown in Figure 9. Additionally, there is no one singular reason LEDs degrade, instead it is a combination of several processes described below.

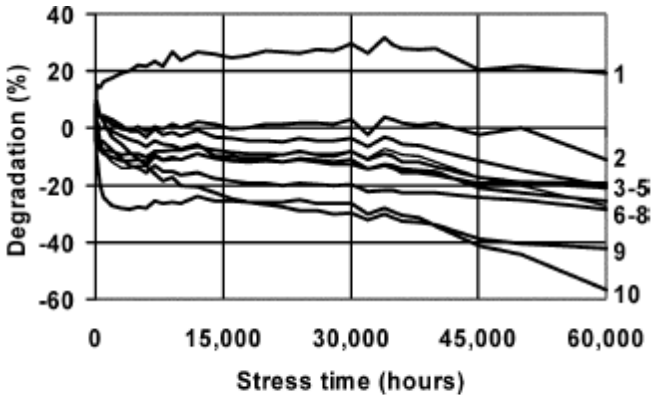

Fig. 3. Degradation data for the 10 wafers in group 2a from Table II out to 60 000 hours of stress at an ambient temperature of 55 °C. Each curve represents a different wafer, and corresponds to the average degradation of 14 lamps.

Figure 9: LED Degradation over time (Grillot, et al. 2006)

1.4.1. Active Region Degradation

There are a variety of ways that the active region's performance can degrade. As it was described above, it is the recombination of electrons and holes that create light, but in fact not all recombinations produce light. Nonradiative recombination creates heat, and typically occurs in point defects and crystal lattice deformations in the active region. Additionally, the electromigration and precipitation of other materials inside the active region can increase nonradiative recombination. Factors that accelerate the development of defects include high current, heating by injected and ambient carriers, and emitted light. (Lee, Hillman, & Kim, 2005)

1.4.2. Thermal Runaway

Thermal runaway is a condition wherein an area becomes damaged because of heat, and this damage causes more heat, which causes more damage, etc. This frequently occurs around areas of nonradiative recombination like point defects in the silicon. It can also occur if the area surrounding the leads becomes an insufficient thermal path, causing a buildup of heat where the lead had previously acted as a thermal sink.

1.4.3. Thermal Fatigue and Shorting

The wire-bond connecting the p-layer with the LED lead is fragile and can cause the LED to catastrophically fail when it breaks. The most common reason for the wire-bond to fail is a differing thermal coefficient of expansion in the materials of the LED. It can also occur if the glass transition temperature of the epoxy encapsulant is reached, either from excessive drive current or high ambient conditions. When the epoxy begins the glass transition, it causes rapid expansion breaking the wire-bond.

1.5. LED Life Test

It is extremely important to know the lifetime of LEDs before using them in a design. However, because of the useful lifetime of LEDs are over 35,000 hours, a full lifetime test would take over 50,000 hours (5.7 years) to complete. The amount of time for a full lifetime test is certainly not acceptable for the fast moving technology world, thus other methods of estimating the useful lifetime of LEDs are employed by manufacturers and researchers. The two most common methods are accelerated life test and the IESNA standard.

1.5.1. Accelerated Life Test

Accelerated life test is a common test among any engineering design to estimate operating life. The goal of this test is to obtain the normal aging effect in a relatively short period of time by operating devices above its maximum ratings. In a LED accelerated life test, LEDs will be driven above their rated current in order to get the degradation effects discussed in the previous section. During the test, brightness, color spectrum, temperature, and other characteristic of the LEDs will be measured and analyzed. LED lifetime researches using accelerated life test done

by Zhejiang University in China and Padova University in Padova drove their 350mA LEDs at 400mA and 500mA respectively. Both of the studies got useful results under 3,800 hours, which is significantly less time than a full lifetime test. (Shen, Pan, & Feng, 2006) (Trevisanello, et al., 2008)

1.5.2. IESNA Standard

Because of the soaring popularity of LEDs and increasing number of manufactures, a standard is needed for estimating lifetime of LEDs. In 2008, IESNA LM-80 was adopted as an industry standard in the United States. IESNA LM-80 defines lumen maintenance testing for LED packages, arrays and modules. Under this standard, manufactures will only need to test the LEDs for 6,000 hours to estimate their useful lifetime. (U.S. Department of Energy, 2008)

1.6. Video Panel Displays

Besides indicators and illumination, another application where LEDs have been very successful is large-scale video displays, like arena video screens and electronic billboards. Previously, projection was the only large-scale method of video displays. LEDs have allowed screens to become much thinner and modular, while also greatly increasing light output. They are even visible in direct sunlight. Annual LED video display sales exceed $41 million. (Dorsch, 2009)

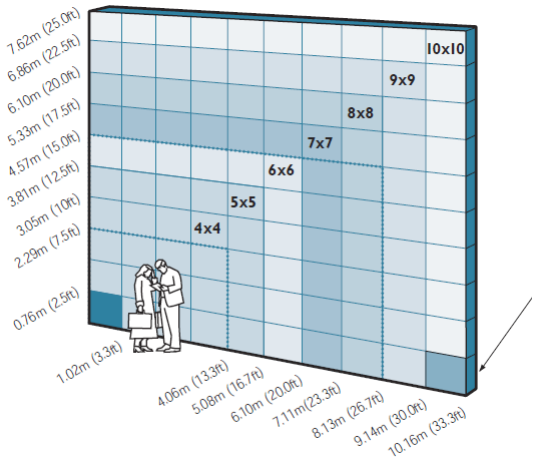

Figure 10: Lighthouse R16 Panel Configurations

The panels used for video applications can vary greatly. They are sold for either fixed installation or modular rental/touring packages. From there, they are differentiated whether they are indoors or outdoors. Pixel pitch is a term used to describe how far apart each pixel, or cluster of red, green, and blue LEDs, are from each other. For indoor applications, the pixels are often spaced as closely as possible, sometimes necessitating the use of surface-mount instead of leaded LEDs. In outdoor applications, panels need to be very large so that they can be seen from long distances. In these environments, pixels are often spaced from 10mm up to 23mm apart. (Daktronics)

Additionally, besides pixel pitch, viewing angles are a critical design feature. As a result, many LED manufacturers produce custom LEDs for video applications with oval dispersions like 100° horizontal by 40° vertical. In this way, light is not wasted shining upwards at the ceiling or sky and it is spread horizontally so that it can be viewed by almost any angle. LED brightness is also a critical decision. For indoor applications, up to 2000 nits are required, whereas the longer viewing distances and direct sunlight outdoors require 5000 nits or more. Nits are a unit of light output in candela per square meter, where a candela is roughly the amount of light a single candle emits in a single direction, weighted by the sensitivity of the eye to various wavelengths.

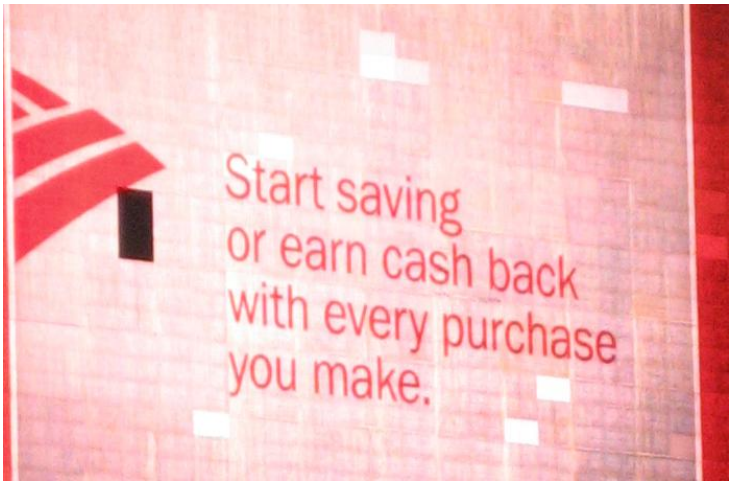

Figure 11: LED Billboard in Time Square

1.7. Calibration

When LEDs were first used as indicators, color accuracy and output degradation were not seen as a problem. However, when used in video displays color accuracy and output are very important. The human eye can see a module-to-module difference of 3% luminance (output) and 1-2nm of color.(Harris S. , 2009) The first generation of LED screens used manufacturer binning to produce uniformity. The trouble is that LED output can vary as much as 40% in their first 500 hours of use, as shown in Figure 9. This results in the quilt-like appearance shown in Figure 11. As a result, many modern LED displays use pulse-width modulation (PWM) to drive each individual LED. With PWM, you gain control of the peak wavelength in addition to intensity. Figure 12 shows the process of correcting a luminance and color shift in a green LED by multiplying it by a 1x3 matrix, however for an entire pixel's correction a 3x3 matrix is used since each LED color depends on the others to generate the correct chromacity. Now, either in the factory or out in the field, full-panel calibration can be performed to correct the uneven degradation of the LEDs.

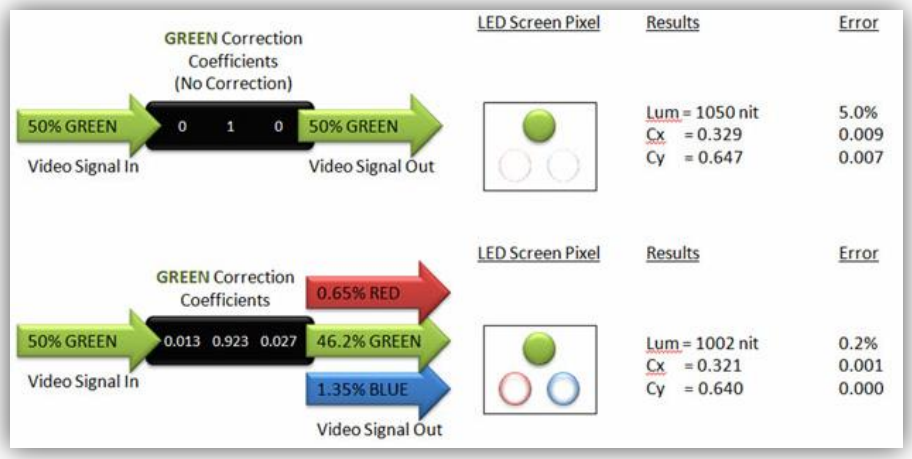

Figure 12: LED Pixel Calibration(Harris S. , 2009)

2. Implementation

Once our research was complete, we began the initial design of our prototype.

2.1. Overall Design

There were two main stages of the design and implementation aspect of our project. The first phase was an LED characterization. As part of this phase, we tested degraded and new LEDs using a Red Tide Spectrometer, provided by the Physics department at WPI. To degrade the LEDs, we stressed three of each color from each manufacturer with a high DC current. After the LEDs degraded, we compared their emission spectrum and intensity to those of a new LED, and determined how the degradation affected the LEDs ability to emit and sense light. The second phase of our design was a final prototype. We used an FPGA to control the user inputs for current and PWM and also to control and manipulate the feedback from an LED acting as a sensor. We used one LED as an emitter and another as a sensor. Both LEDs were connected to the driver circuit, and could be toggled in an alternating fashion. So, when we wanted to drive one LED, the other LED would be connected to the FPGA and act as a sensor. A basic overview of our final implementation can be seen in Figure 13.

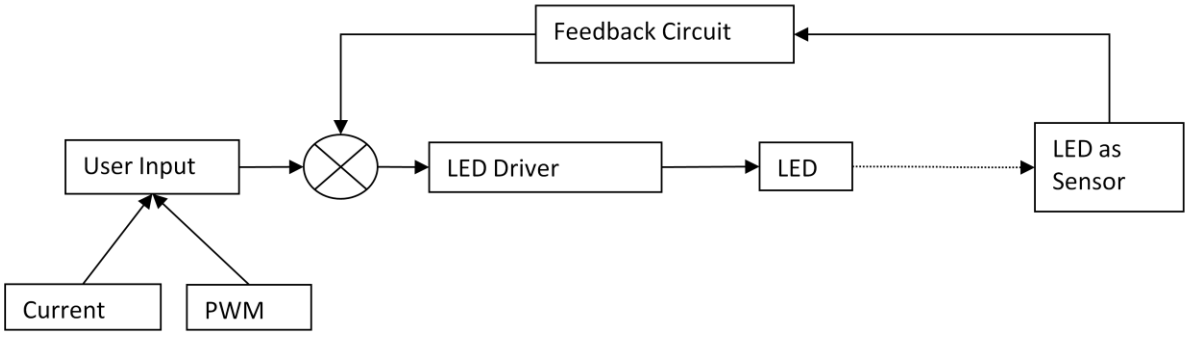

Figure 13: Final Implementation

2.2. LED Selection

LEDs that are used in outdoor video displays were chosen for this project. Although it would be ideal to use the same LEDs the outdoor video display manufacturers use, but they are very protective of such information. Despite this setback, we investigated products from Daktronics,

Mitsubishi Electric, and Lighthouse Technology and came up with a selection of LEDs which are similar to ones inside an outdoor video display.

Both discrete and surface-mounted (SMD) LEDs are used in outdoor screens. Due to the large size of outdoor display panels, the bigger discrete LEDs are the more popular choice among manufacturers. Additionally, the package of discrete LEDs is easier for us to work with than the surface-mounted. On top of the decision between discrete and surface-mounted, there are different types of discrete LEDs. Discrete oval LEDs are often used due its oval shaped radiation pattern. Since it is most desirable for an outdoor video display to have a wide horizontal viewing angle, oval LEDs would be a good choice. Lastly, high luminous intensity is also important in order for far viewing distance and visibility under sunlight.

With those criteria, we selected fitting models made by leading manufacturers Avago, Cree, Nichia, and Optek. The table below is the list of LEDs we have chosen for this project.

Model	Mfg.	Package	Color	Dominant Wavelength	Horizontal Viewing Angle	Vertical Viewing Angle
HLMP-HB65	Avago	5mm Oval	Blue	470	100	40
HLMP-HM65	Avago	5mm Oval	Green	525	100	40
HLMP-HG65	Avago	5mm Oval	Red	626	100	40
NSPB546DS	Nichia	5mm Oval	Blue	470	110	40
NSPG546GS	Nichia	5mm Oval	Green	525	110	40
NSPR546HS	Nichia	5mm Oval	Red	626	110	40
C5SMF-BJS	Cree	5mm Oval	Blue	470	100	40
C5SMF-GJS	Cree	5mm Oval	Green	527	100	40
C5SMF-RJS	Cree	5mm Oval	Red	621	100	40
OVLJBGD8	Optek	5mm Oval	Blue	470	100	40
OVLJGGD8	Optek	5mm Oval	Green	525	100	40
OVLJRGD8	Optek	5mm Oval	Red	626	100	40

Table 1: LED Selections

2.3. Current Source

Since LEDs are current driven devices, they are best driven by a current source. For this project, we want to vary the emission intensity of the LED by adjusting the level of supply current. Therefore, we need an adjustable current source. There are adjustable current source ICs in the market, but they either do not provide the 250mA we need or require external component changes for current varying. We decide it would be best for us to design an adjustable current source.

The circuit shown in Figure 14 is an adjustable current source controlled by voltage signal form a FPGA controller. In this design, the BJT act as a current controlled current source. It controls the amount of current flow from the power supply to ground depending on the amount of current that is applied to its base. When the base voltage is higher than the emitter voltage, the BJT will be on and current will flow from the +5V rail to ground. This current will drive the LED connected between the +5V rail and the collector of the BJT.

In order to control the current flow, a feedback loop is need on the BJT. We accomplished this by designing a feedback system consisting of a voltage follower and a non-inverting amplifier. The supply current flow through the BJT is detected as voltage by a 1Ω resistor placed at the emitter of the BJT. This voltage is amplified by the non-inverting amplifier to represent the 0mA to 250mA of supply current as 0V to 2.5V. The amplified voltage is then fed to the minus pin of the voltage follower. The plus pin of the voltage follower takes voltage signal from the FPGA. Due to the nature of the voltage follower, the voltage of its plus, minus, and output are the same. Thus it allows us to control the BJT's gate voltage and monitor the feedback voltage.

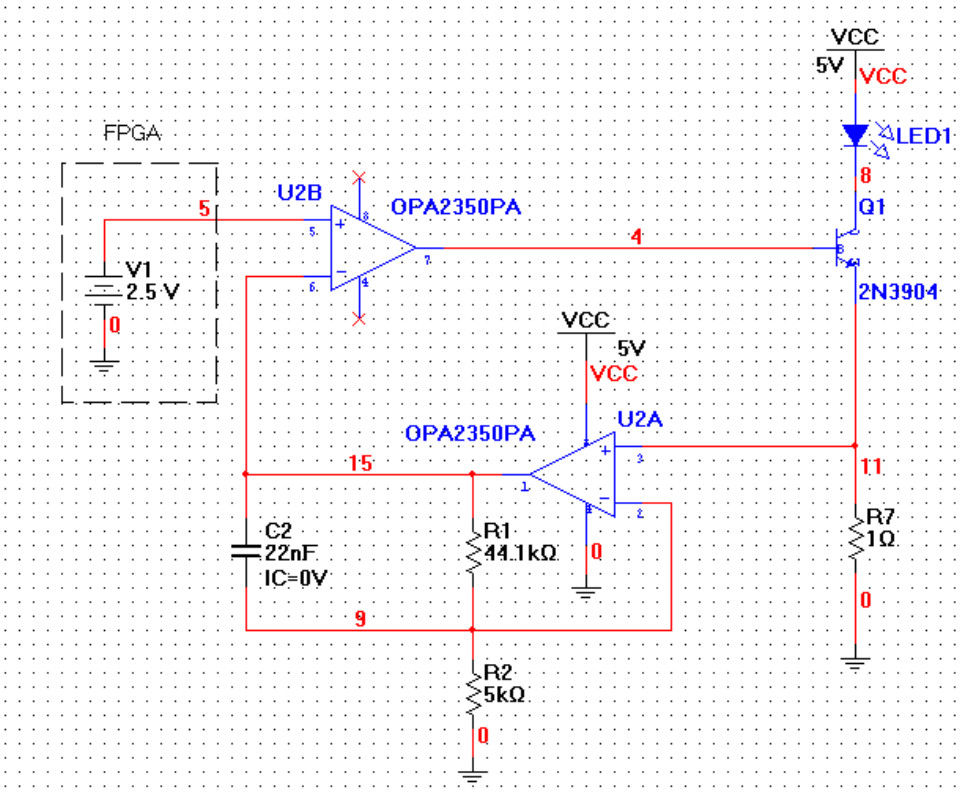

Figure 14: Adjustable Current Source

We have chosen the OPA2350PA operation amplifier because of its ability to run in "single rail" and have enough bandwidth for our application. This allows us to have a +5V rail and a ground rail instead of a +5V rail and a -5V rail without doing any extra configurations. The non-inverting amplifier is set to have a gain of 9.82. Due to an oscillation problem, we added a capacitor in parallel to feedback resistor R1 to make a low pass filter with cutoff frequency at around 164Hz.

2.4. MOSFET Driver

In order to pulse width modulate our LEDs, we based our circuit around the layout concept below in Figure 15. This circuit allows us to sequence through the LEDs one at a time, and also isolate each LED for sensing by connecting the FPGA pins to each of the common buses. The downside of this circuit is that it requires very fast and precise PWM pulse control. For example, the Lighthouse Technologies R16i has 16,384 levels of intensity. (Lighthouse Technologies Ltd., 2009) If we give the below panel of 9 LEDs a refresh rate of 120Hz, that means each LED will

be on for 3.7ms if at full intensity. If we subdivide the 3.7ms down into the 16,384 intensity levels, this results in a minimum pulse size of 842ns, or 1.19MHz switching speed.

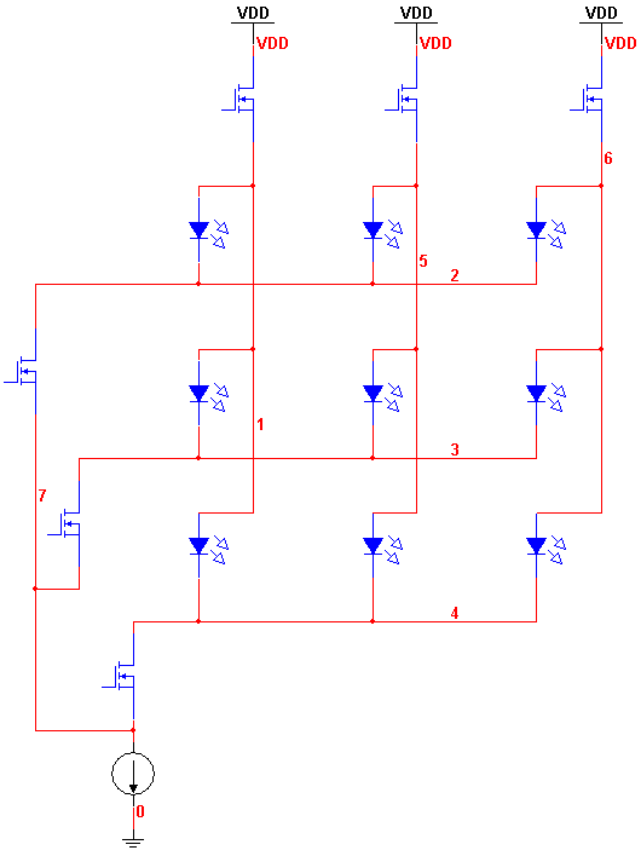

Figure 15: LED Switching Configuration

For the switch we chose to use an NMOS transistor because of its speed and greater availability compared to PMOS counterparts. We selected the BS-170 from ON-Semiconductor because it had exceptional speed performance and an adequate current rating and on-resistance. The tradeoff for greater speed comes at the cost of a gate drive voltage that needs to be greater than the +5V rail. Since our project is a bench-top experiment and since the target market does not have any power restraints like batteries, it was sufficient for us to create a gate driving circuit that runs off of a higher rail. In our case, that higher rail is at +15V.

The first device that we tested was the ON-Semiconductor MC34151 MOSFET driver. This is an integrated circuit that accepts logic inputs and ties the output to either V+ or ground

depending on the logic input as shown in Figure 16. The datasheet specifies rise and fall times <= 15ns with a load capacitance of 1000pF (which is much greater than the BS170's 60pF input capacitance), which exceeds our requirements.

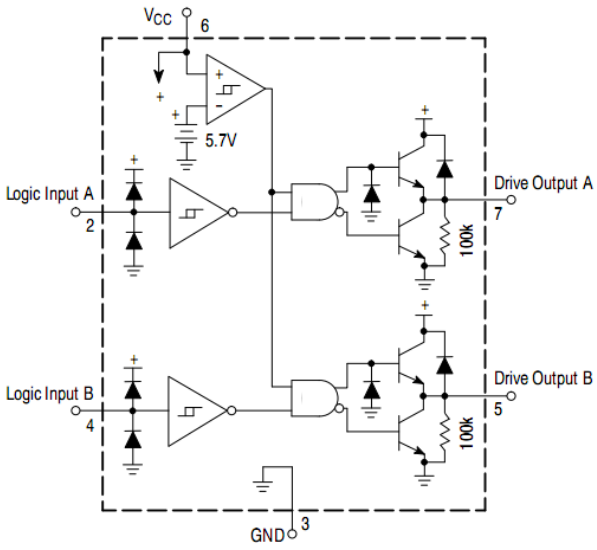

Figure 1. Representative Block Diagram

Figure 16: MC34151 MOSFET Driver

When we built our first prototype on a solder-less prototype board (breadboard), we experienced some very strange anomalies, shown in Figure 17. While the circuit was usable at the 250kHz we had designed it to operate at, we were unhappy with the result. The bottom trace is the voltage at the low-side of the LED, so therefore when the square wave was low, the LED was on. However, during the output anomaly the LED did not have enough current to turn on, and so as the frequency of the PWM signal increased the amount of low time became dominated by the anomaly until the LED simply never turned on.

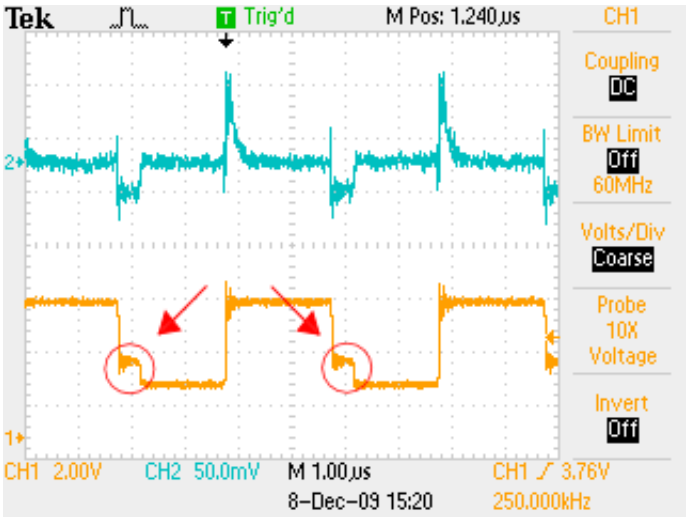

Figure 17: Output anomaly

Because the MC34151 was a "black box" that we had no control over, we were led to believe that it was the cause of the problem. In order to test this theory, we created the circuit driver shown below in Figure 18. It operates by driving the bases of an NPN and a PNP transistor. When the logic input is low, the gate-to-source voltage of NMOS Q3 is great enough that it turns on, pushing +3V into the common bases of the BJTs, causing the 2N3906 to "turn on", discharging the gate capacitance. When the logic input is high, the gate-to-source voltage of Q3 is not enough to turn on, so the common bases are pulled up to +15V through R2, turning on the 2N2222. While this circuit is not capable of draining the gate capacitance below 0.7V, it is more than enough to completely cutoff the MOSFET. The resulting driver operated nearly identically to the MC34151, except with a cleaner square wave with less overshoot and ringing. It operated well up to 6 MHz on a breadboard.

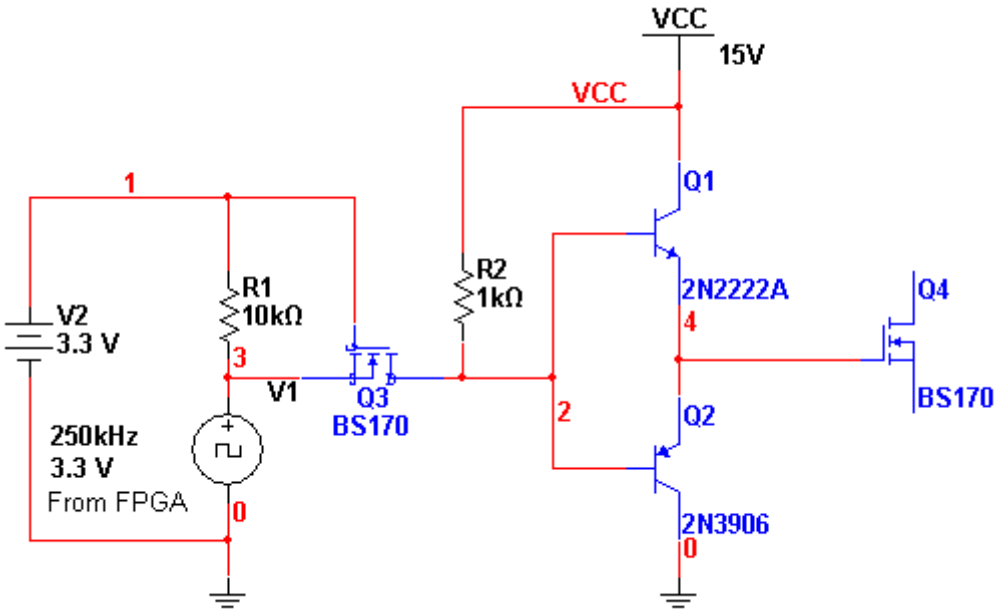

Figure 18: Discrete Mosfet Driver

Despite the new driver, the "knee" in the output still remained. After playing with a large variety of filtering capacitors on every part of our circuit, it was eventually discovered that the voltage divider we were using to simulate the DAC output of the FPGA, shown in Figure 19, was being excited by the stray capacitances of the breadboard. Tying a .047 µF capacitor across the non-inverting input solved the problem.

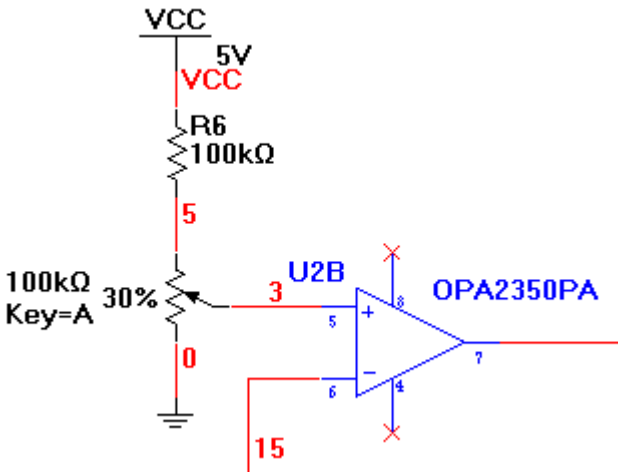

Figure 19: High Impedance Point

2.5. Lifetime Testing

To perform out lifetime testing, we needed to degrade at least one of each LED of each color from each manufacturer. In consideration of time constraints, we chose to degrade more than one LED at once. If we had more time in the project, a more precise and detailed method of degradation would have been used. Our lifetime testing current driver can be seen in Figure 20. We placed twelve LEDs in series, three of each color for each manufacturer, and degraded them simultaneously with a high DC current. In this setup, we had to run the degradation setup three times to degrade the red, green and blue LEDs separately. We used the same current driver circuit, replacing the high impedance point with a power supply so we could obtain precise control of the current flowing through the LEDs. The only other difference was the addition of a BS170 n-channel MOSFET in series with the LEDs. This MOSFET was added so that we could "turn off" the current source once the current of the sensing LED had reached a certain threshold. We also added a reverse biased LED to sense the current in one of the emitting LEDs, which was connected to the transimpedance amplifier.

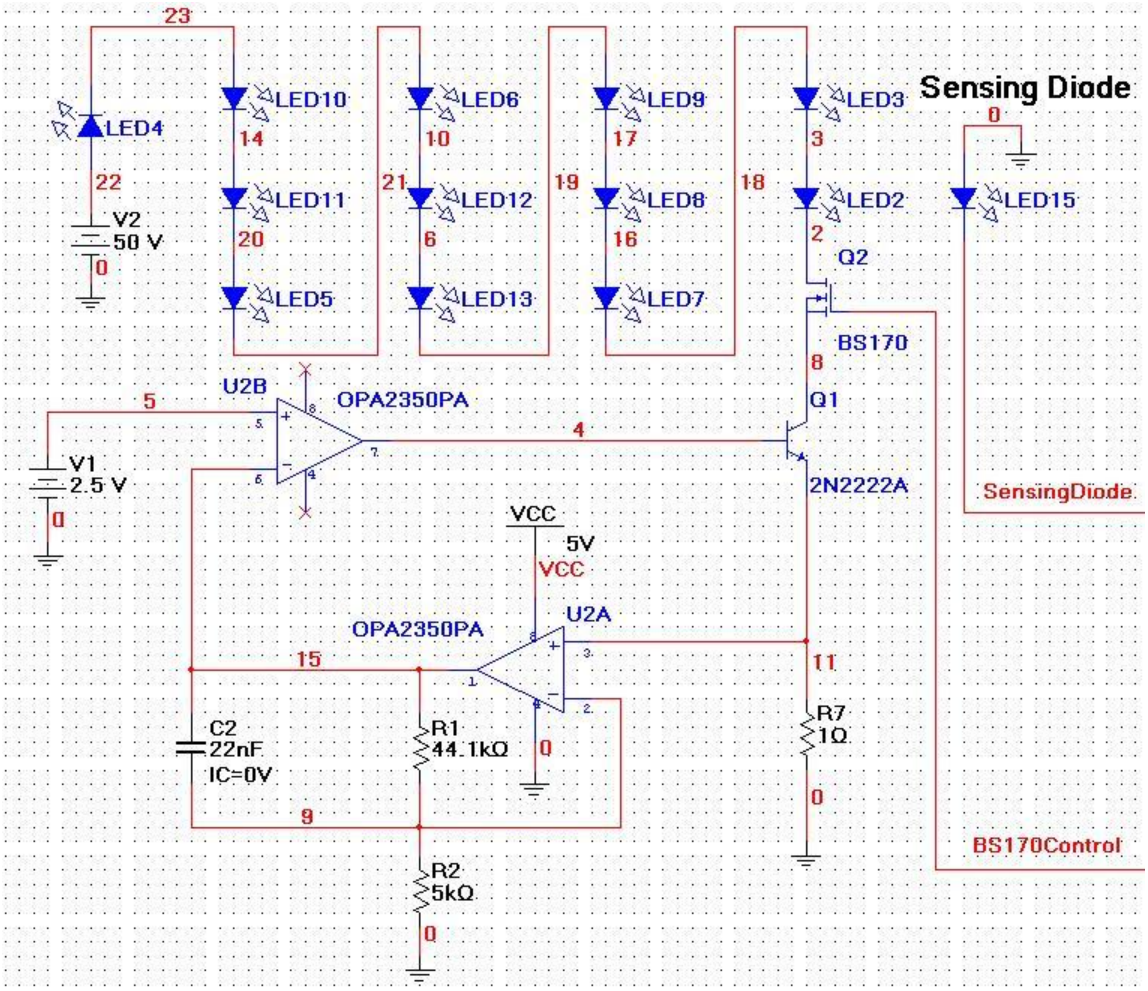

Figure 20: Lifetime Testing Current Driver

We also had to develop a trigger circuit to turn off the current driver, which can be seen in Figure 21. As part of the trigger circuit, we needed to determine the current being produced by the sensing LED. We decided to use a transimpedance amplifier, which would convert a current created by the sensing LED into a voltage. For this transimpedance amplifier, we needed an operational amplifier that had a high input impedance to draw as little current as possible and null offset pins to eliminate the DC bias of the circuit. We eventually chose the TL081BCP, as it had a JFET input stage with an input resistance of 10^{12} Ω and included offset pins. Constructing this circuit, we choose R9 to obtain a gain of 100,000 V/A and connected the null offset pins as recommended by the datasheet. Finally powering up the circuit, we tuned the potentiometer until we obtained an output of about 0V with the inverting input grounded. We also verified that the gain was 100,000 V/A as expected.

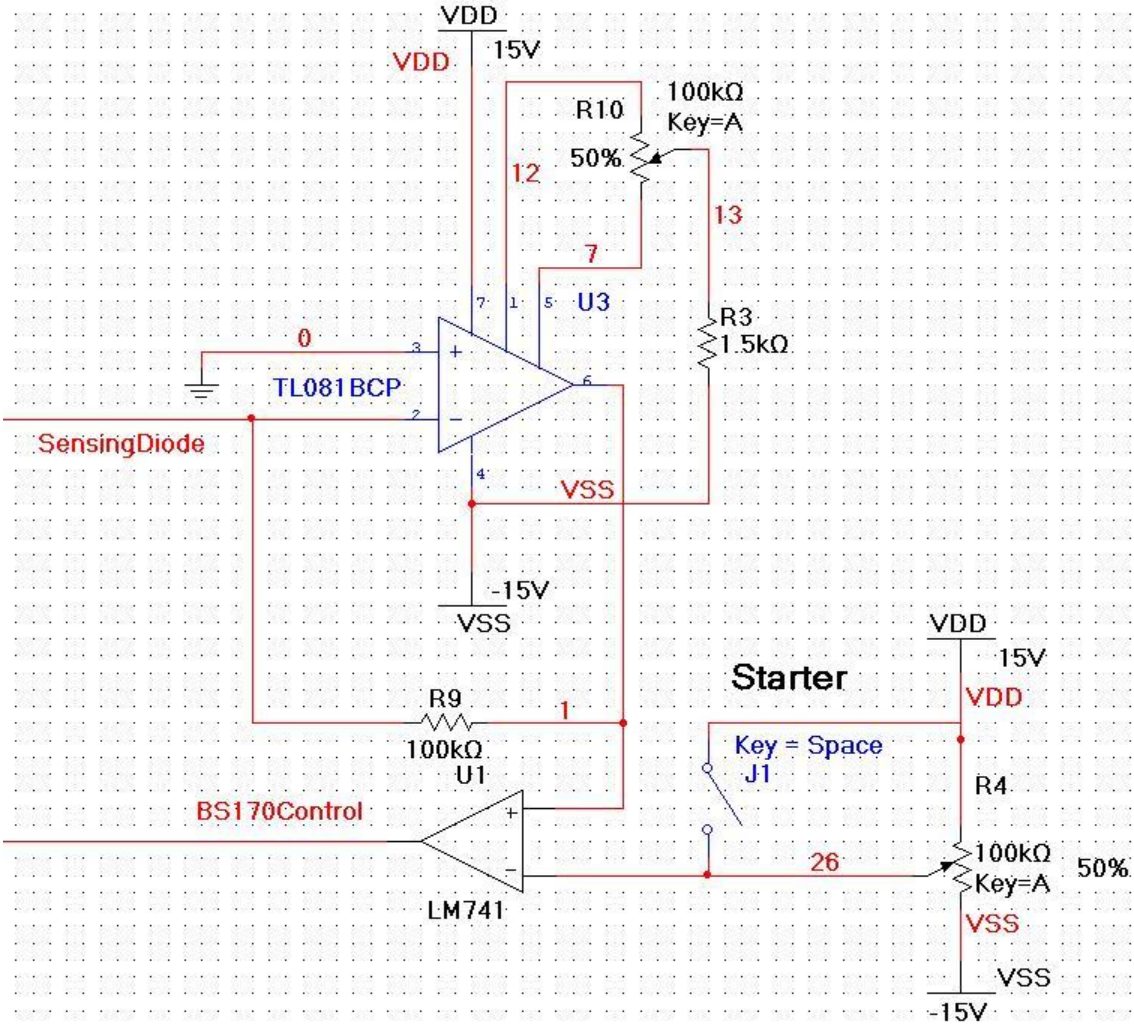

Figure 21: Lifetime Testing Trigger Circuit

However, we still needed a way to control the gate of the BS170. After considering several options, we decided to use an LM741 as a comparator. The output of the LM741 would go low once the output of the transimpedance amplifier passed below the threshold, which we could set by changing the value of potentiometer. Once this output went low, the BS170 would turn off and break the current driver circuit.

After running all three tests, we obtained the results seen in Figure 22, observing the voltage at the non-inverting input of the LM741 comparator. There are several observations that can be made about this data. The first observation is that while the blue and green LEDs had a steady

decay over time, the red LED actually increased in brightness before eventually reaching the threshold. While this seems unusual, our research has shown that the intensity could actually increase over time (see Figure 9) before finally degrading. Next, we can see that the blue LEDs took about four days to degrade while the red and green LEDs took about two days to degrade. This time difference is due to the fact that we ran the blue LEDs with a current of 50mA, then increased the current to 100mA for the last two colors. Another observation is that of the blips in each data set. These irregularities indicate that we turned the power supply off and on. The jump in the blue LED data indicates when we added a heat sink to the voltage regulator in order to increase its thermal performance. Lastly, the three different levels indicate that each color of LED had a different intensity level. Overall, we can say that these LEDs are degraded and are ready to be tested by the spectrometer and used as detectors and emitters in our final testing.

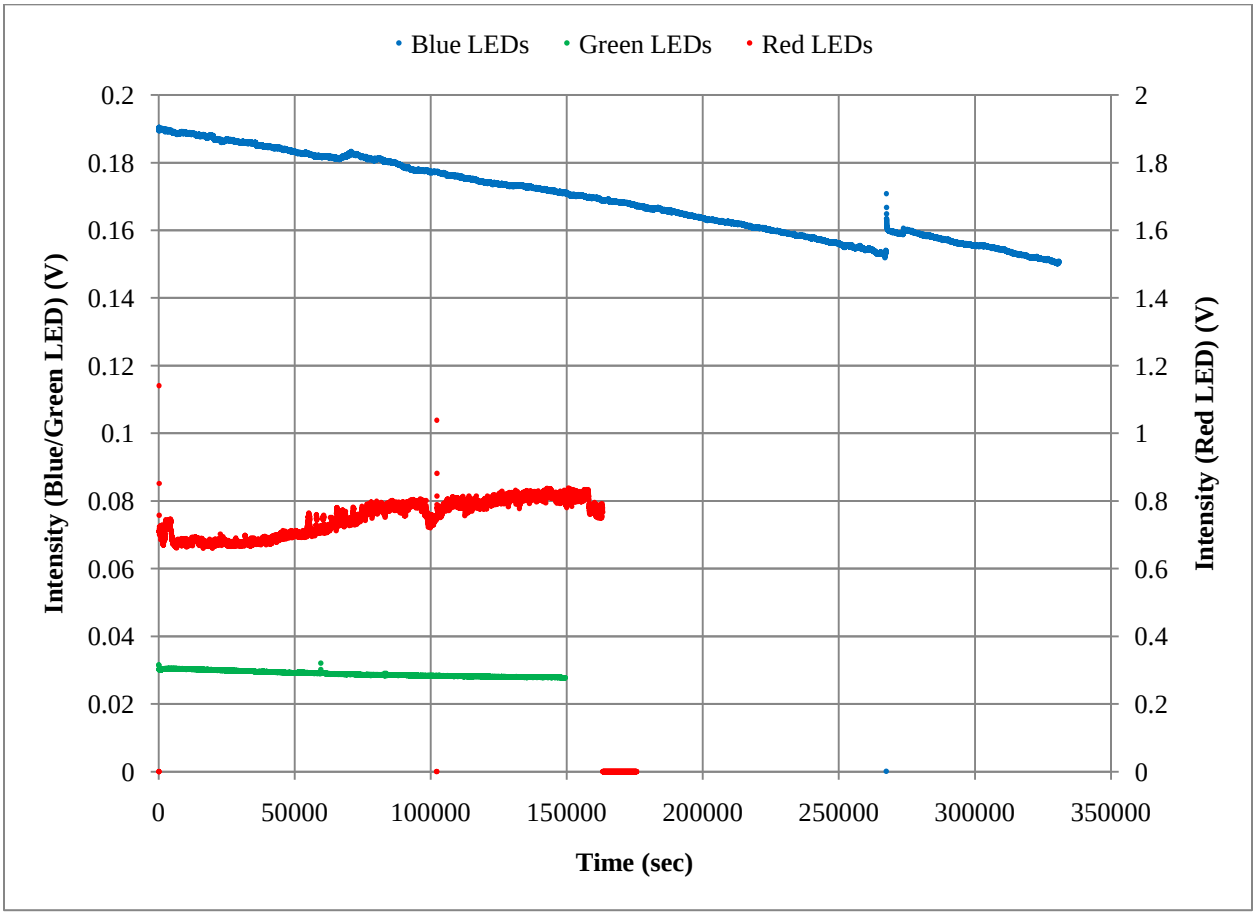

Figure 22: LED Lifetime Testing Data

2.6. Control

For our device we have chosen to implement all of our control system with an FPGA. We found that the speed and number of I/O pins on the FPGA was more favorable for our target market than a microcontroller. More specifically, we chose the Xilinx Spartan-3E FG320 because it offers 232 I/O pins and operates at 50MHz. The very high I/O count is very important when dealing with very large arrays of pixels, and with minimum duty cycle pulses at 6 MHz, standard microcontrollers running at 16MHz would struggle to keep up. The Spartan-3E we are using is mounted on a Nexys2 development board from Digilent Inc because everyone on the team was familiar with the board.

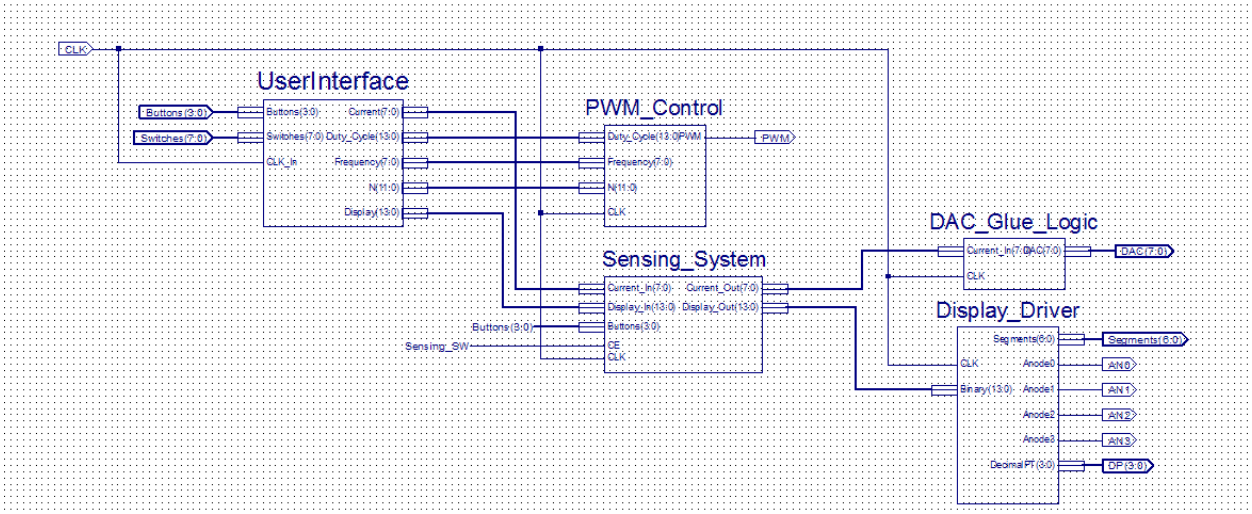

Figure 23: FPGA Top-Level Layout

The control system has been broken down into five sections shown in Figure 23. The User_Interface block takes the input switches and buttons, changes input modes, and outputs the value currently being edited. The PWM_Control block interprets the values of the User_Interface outputs and constructs the PWM signal. The DAC_Glue_Logic interfaces the output of the user interface with the external DAC. The Sensing_System block switches the circuit from driving the LEDs to sensing with them. It performs two measurements, one against a new LED and another against an aged LED, and determines an offset. Finally, it applies the correction to the Current bus that it is passed through. And finally, the Display_Driver converts an unsigned binary number into four base-10 digits and adapts them for the Nexys2.

2.6.1. User Input Interface

The user interface block allows our device to be programmed without the aid of a computer. It has four editing modes, one for each parameter of our output. The current, duty cycle, frequency, and n mode are each selected with one of eight sliding switches, and only one mode may be active at a time. In each editing mode, each button represents a different increment value, and a switch switches between addition and subtraction from the current value. The table below shows the button designations and output range values.

Mode	Range	Button 3	Button 2	Button 1	Button 0
Current	0-255mA	1mA	5mA	10mA	100mA
Duty Cycle	0-100%	1%	5%	10%	50%
Frequency	0-255kHz	1kHz	10kHz	50kHz	100kHz
N	0-4095	1	10	100	1000

Table 2: Button Designations of FPGA

The implementation of this block is mainly focused on responding to the toggles of switches and buttons presses. At the beginning of the input stage, each of the editing modes has its own accumulating module directly connected to the switches and buttons. Each module is enabled by its corresponding switches implemented using NOR gates. The NOR gates logic also protects the system from enabling more than one mode at a time. Once enabled, the accumulating module, consisting of a multiplexer and a 16-bit accumulator, will response to any button press and calculate the input value of the respective mode.

2.6.2. Display Driver

The display driver circuit inputs a single unsigned binary number and converts it to a format that can be output to the Nexys2's LED displays. Figure 24 below shows the configuration of the Nexys2 7-segment displays. The cathodes of each digit are controlled simultaneously while the anodes are sequenced through for individual control. In order to display our number we are required to separate the binary input into the four separate base-10 numbers on the display. From there we can sequence through the digits with the anode pins and output the results.

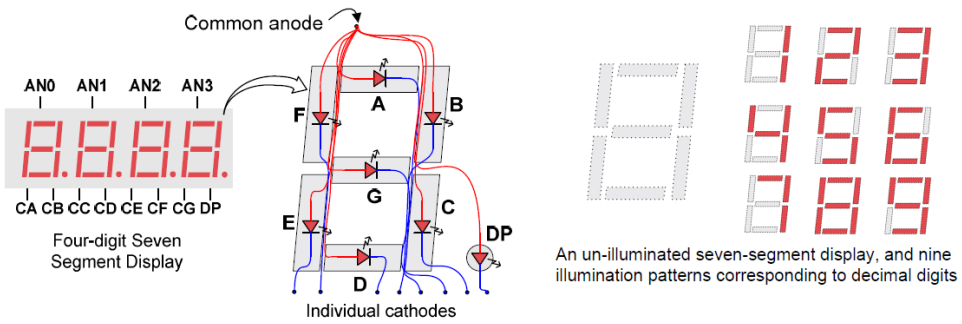

Figure 24: Nexys2 7-Segment Displays (Nexys2 FPGA Board, 2008)

We generate the four separate decimal numbers by feeding the binary value to be displayed to a 16-bit counter that triggers four cascaded modulo ten counters. This is shown in Figure 25. The 16-bit counter is reset by a predetermined maximum value or a user input. The four cascaded modulo ten counters, shown on Figure 26, turn the binary input value into decimal representation and keeps track of the one, ten, hundred, thousand digit. The four decimal digits can then be used for the display driver.

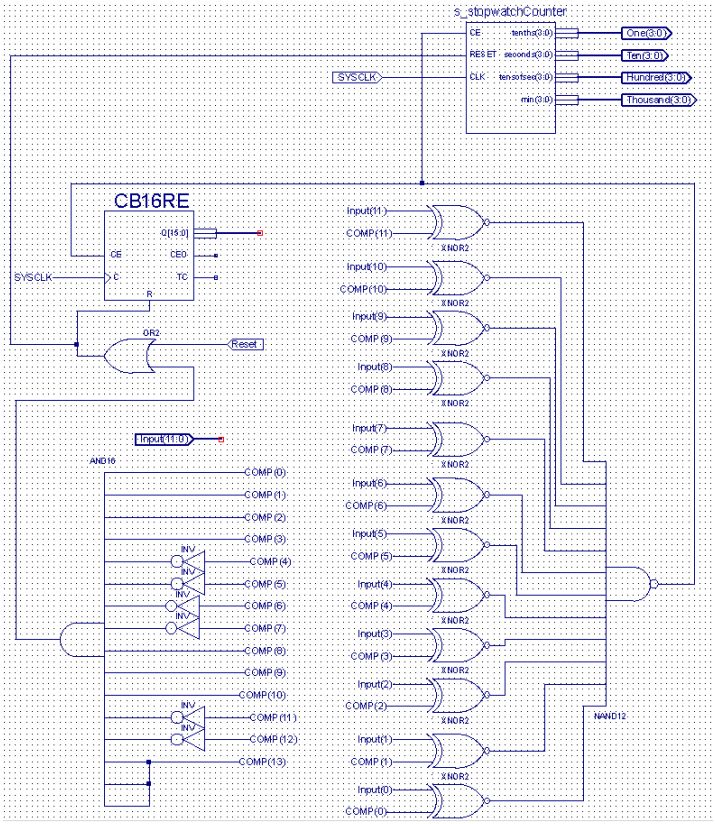

Figure 25: Binary Input to Separate Decimal Digits

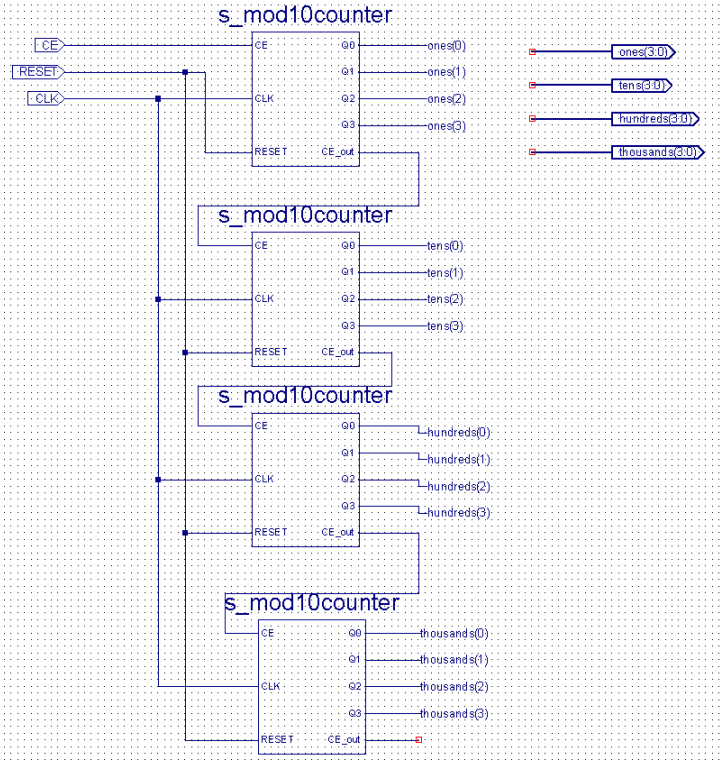

Figure 26: Four Cascaded Modulo Ten Counters

Once the decimal digits are ready, they will be passed into the seven segment LED driver shown in Figure 27. Since only one digit can be active at one time, the decimal digits are input into a multiplexer. The multiplexer output each decimal digit in order to the seg_hex module. This module translates the digit into segments on the seven digits display. At the end, the anode driver multiplex through the four digits on the seven segment display at 10kHz to display the decimal digits.

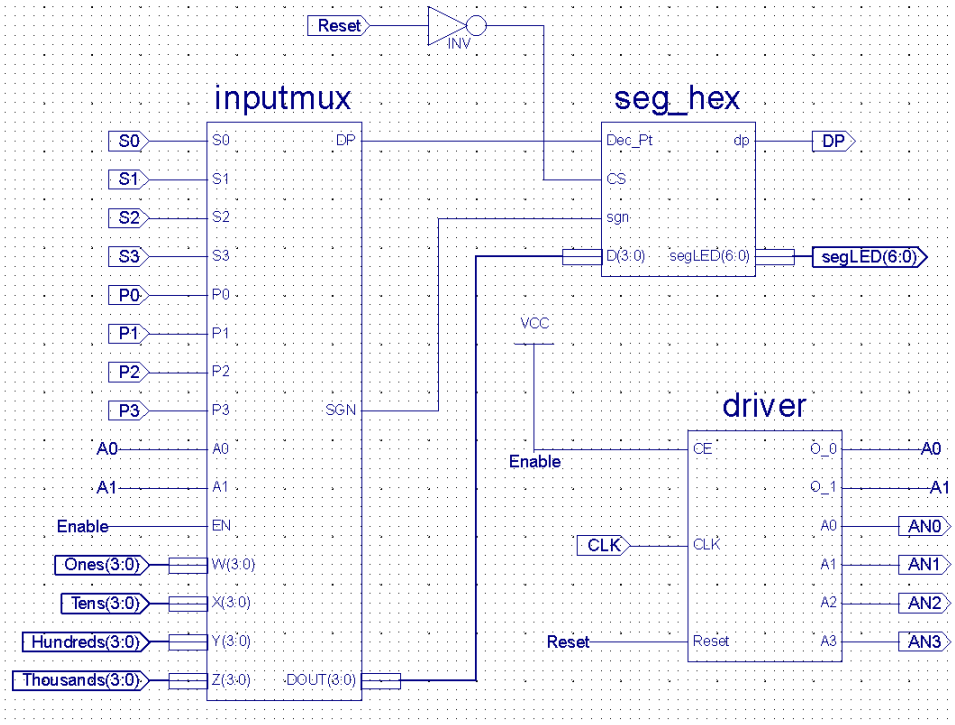

Figure 27: Seven Segment Display Driver

2.6.3. DAC Glue Logic

The current control block converts the user inputted current level to an analog signal for the adjustable current drive through the Digilent Pmod DA1 Digital To Analog Module Converter. The DA1 DAC is an external module attached to one of the expansion ports provided on the FPGA board. The driver for the DA1 DAC is provided by Digilent as shown in Figure 28. The inputted current is fed into DATA1 of the driver to be converted. D1, D2, CLK_OUT, and nSYNC are mapped to the physical pins connected to the DA1 DAC. Since we want the DAC to convert the current continuously, we tied DONE to START. Therefore, as soon as a conversion is done, it will trigger the next conversion to start right after.

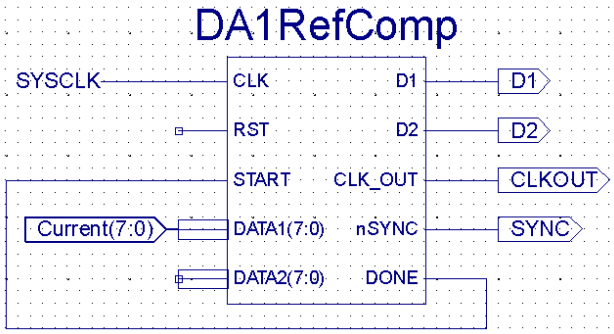

Figure 28: Pmod DA1 DAC Driver

When we tested the DAC implementation we found that it had an output offset which caused very high error with low currents. We originally tried to implement a gain correction, but found that it was going to cause much more error at higher currents. Instead, we found that a software offset was a more accurate fix. Figure 29 below shows the original percent error on the current source and the calculated error with a constant software offset of +5mA.

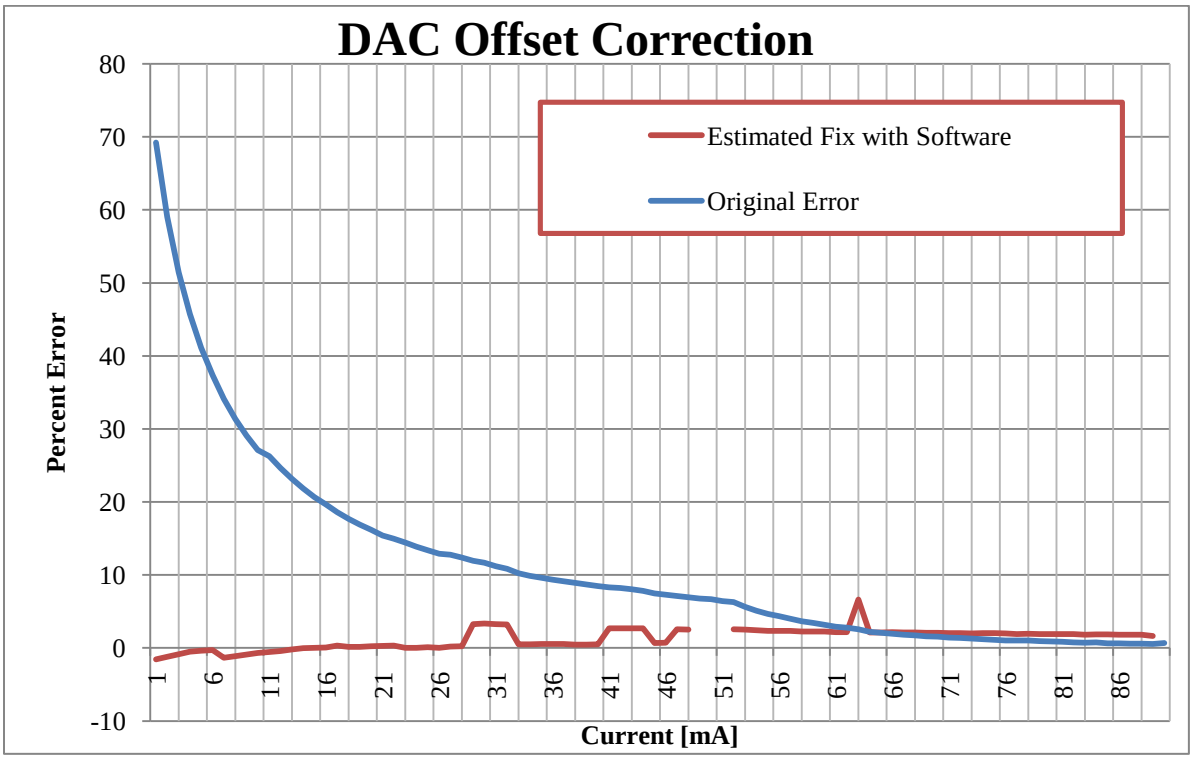

Figure 29: DAC offset error and correction

2.6.4. PWM Control

The PWM control block converts several unsigned binary inputs into a single PWM output pin. The different components of the PWM output are shown below. The duty cycle controls how long the LED remains on during its window of opportunity. The frequency controls how often the active LED in the array changes, in Hertz. And finally, N determines the total number of LEDs that need to be sequenced through in the array before it starts over at the beginning.

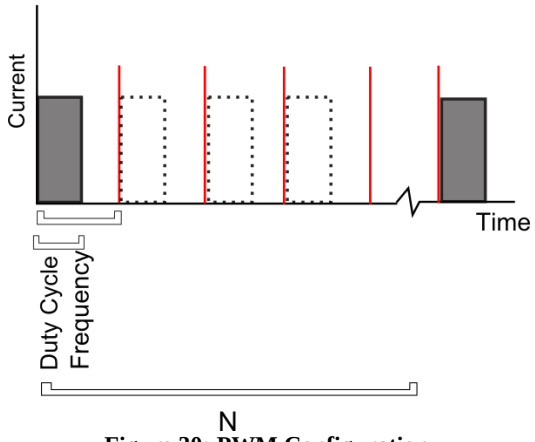

Figure 30: PWM Configuration

The overall design of the PWM block includes a floating point math module and a counter to produce the physical PWM waveform. The floating point math module takes the desired frequency, duty cycle and N and calculates the on and off time of the LED based on those parameters. After the on and off times are determined, the PWM counter counts to the on and off time values to produce the PWM waveform. Figure 31 illustrates the overall design.

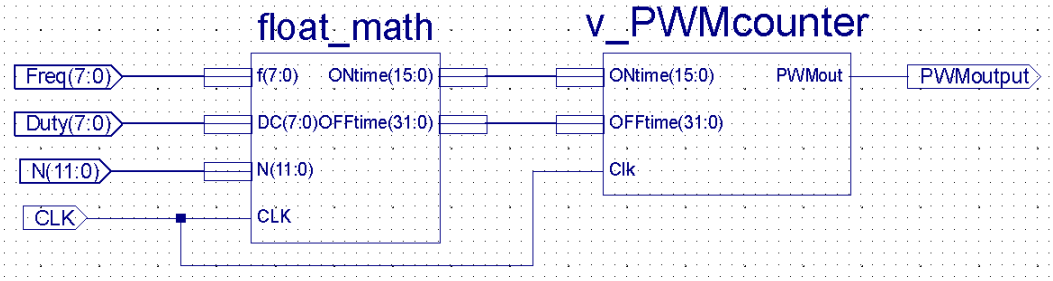

Figure 31: PWM Overall Schematic

The floating point math module is mostly made up of many LogiCore floating point operation modules provided by Xilinx. Figure 32 is the schematic of the float_math module. The 8-bits frequency and duty cycle, and the 12-bits N inputs are first passed into the v_const module. v_const has three functions. First, it zero pads the three parameters to 32-bit, because all of the LogiCores require 32-bit inputs. Besides padding, the v_const module also creates 32-bit floating point constants of 50,000,000, 1,000 and 100 for the ease of later calculations. Lastly, it calculates (100 – duty cycle) and outputs the result in 32-bit format. After the parameters are padded by v_const, they will be converted from fixed point to floating point representation by LogiCore FixedtoFloat.

Once all the numbers are ready for calculations, we used the add, multiply, and divide LogiCore modules to implement equations to calculate on and off time. The two equations are:

$$On\ Time = \frac{50MHz}{freq_{input} * 1000Hz} * \frac{DutyCycle_{input}}{100}$$

$$Off\ Time = \left(\frac{50MHz}{freq_{input} * 1000Hz}\right) * \left((N-1) + \frac{100 - DutyCycle_{input}}{100}\right)$$

50MHz is the system clock. The inputted frequency is multiplied by 1000 to convert the number to kHz. The system clock is divided by the adjusted input frequency to determine the number of system clock cycles needed to produce one period of the desired frequency. This number will be used to calculate the on and off time. For on time, it is multiplied by the percent duty cycle to generate the number of system clock cycles the LED will be on. For off time, it is multiplied by the sum of number of wait period, N, minus one and the rest of the duty cycle. Once the on and off times are calculated, they are both converted back to fixed point. Before sending the two numbers out to the PWMcounter, the on time is truncated to a 16-bit number.

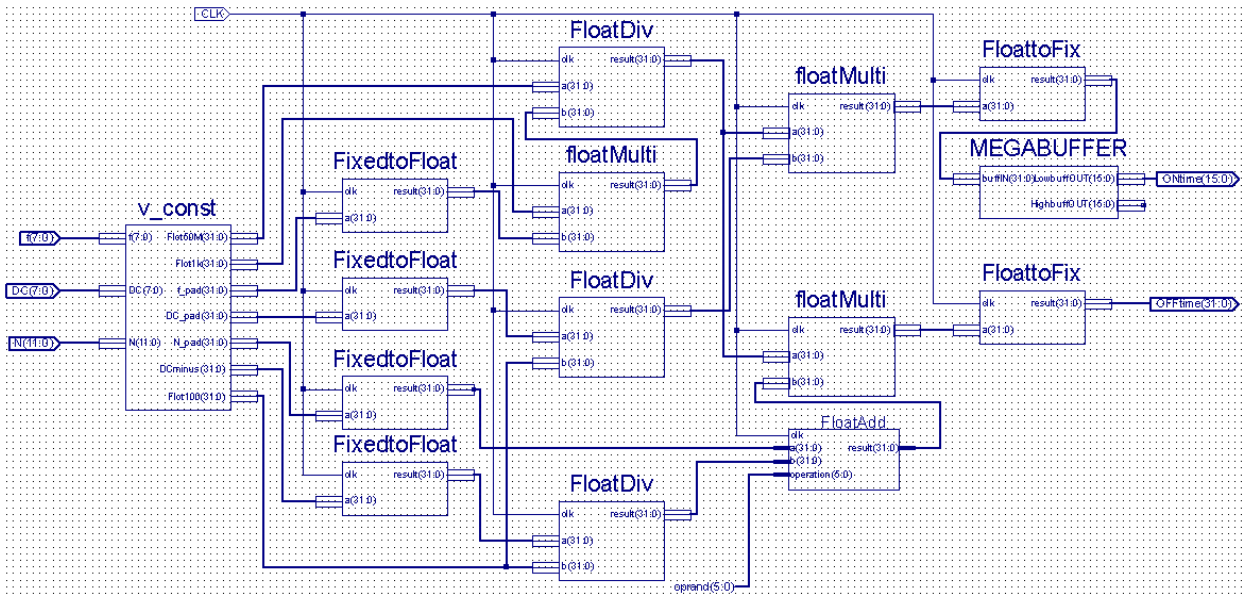

Figure 32: Schematic of float_math

v_PWMcounter is implemented in VHDL, shown in Figure 33. It is mainly a process that counts every clock cycle while keeping track of on and off time. This process is triggered by every rising edge of the system clock. It first checks if the PWM is in on or off mode (initialized to on mode). In on mode, the output of this module is set to high and counter_on is increased by one on each run. Once counter_on equals ONtime calculated in the float_math, the process changes to off mode. In off mode, the output is set to low and counter_off is increased by one on each run. Similar to on mode, the off mode compares counter_off and OFFtime calculated in the last module to determine the next mode.

```
begin

   PWMout <=  tmp_clk;

   process(Clk)
      variable counter_on:integer range 0 TO 65536;
      variable counter_off:integer range 0 TO 50000000;
      variable mode : integer := 1;
   begin
      if Clk'event and Clk = '1' then
         if mode = 1 then
               if counter_on = ONtime then
                  tmp_clk <= '0';
                  mode:= 0;
                  counter_off := 0;
               end if;
               counter_on := counter_on + 1;
         else
               if counter_off = OFFtime then
                  tmp_clk <= '1';
                  mode:= 1;
                  counter_on := 0;
               end if;
               counter_off := counter_off + 1;
         end if;
      end if;
   end process;

end Behavioral;
```

Figure 33: The Main Loop of v_PWMcount

2.6.5. Sensing System

During design and testing we used the transimpedance amplifier described by Section 42.5 to measure the current generated by each LED. While this provided us with accurate and absolute results, it would be impractical to create a transimpedance amplifier with a gain greater than 100,000 for each LED in a video display. Instead, we implemented a method described in the Altera White Paper WP-01076-2.1(Camarota, 2009), which simply uses two tri-state digital logic pins to measure the relative amount of light striking an LED.

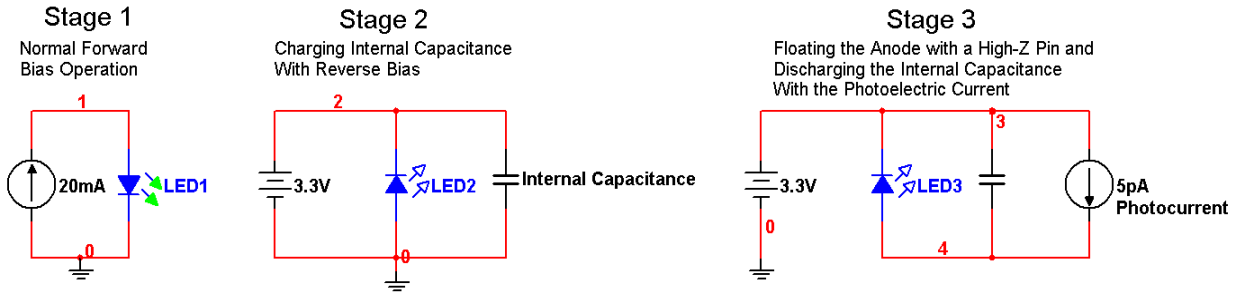

Figure 34: Measuring Photocurrent With Digital Logic

Figure 34 above shows the three different stages of the LED operation. Stage one is the normal stage when the LED is being used as an emitter. During this stage, the FPGA pins that are connected to the anode and cathode of the LED are in high impedance (High-Z) mode to protect themselves from potentially high voltages. In stage 2, the LED is reverse-biased so that the internal capacitance is charged. The internal capacitance is formed by the charge separation of the depletion region, and is on the order of picofarads.

Stage 3 is when the actual measurement occurs. The anode of the LED is disconnected from the charging voltage source. When light strikes the diode it excites a photocurrent from the cathode to the anode. This current slowly discharges the internal capacitance and raises the anode voltage from 0V to 5V. If you measure the amount of time it takes for the anode to rise from 0V to the digital logic threshold, you can calculate the relative amount of light striking the diode. Figure 35 below shows the anode voltage over time. The upper horizontal cursor is highlighting the logic threshold, and the ΔX value is the amount of time the counter will run.

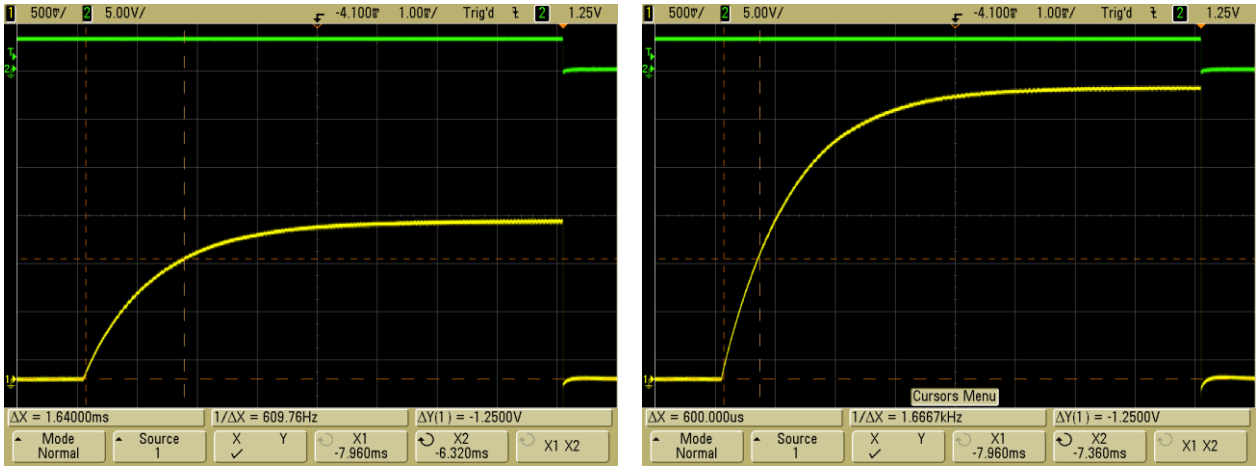

Figure 35: LED Anode Rise Time of Two Different Amounts of Light

We implemented this design using a three state Finite State Machine corresponding to the three stages described in Figure 34. In the schematic below in Figure 36, Q0 refers to Stage 2 and Q1 refers to Stage 3. The lower counter sets the minimum amount of charging time. The center counter is a timeout counter that resets the state machine if there was not enough light striking the LED to trigger the threshold. And finally, the top counter is the intensity measuring counter.

It only counts if it is in stage 3 and the LED anode is still logic 0. Finally, when the anode transitions to logic 1, the output Done will trigger later conversions and display resets.

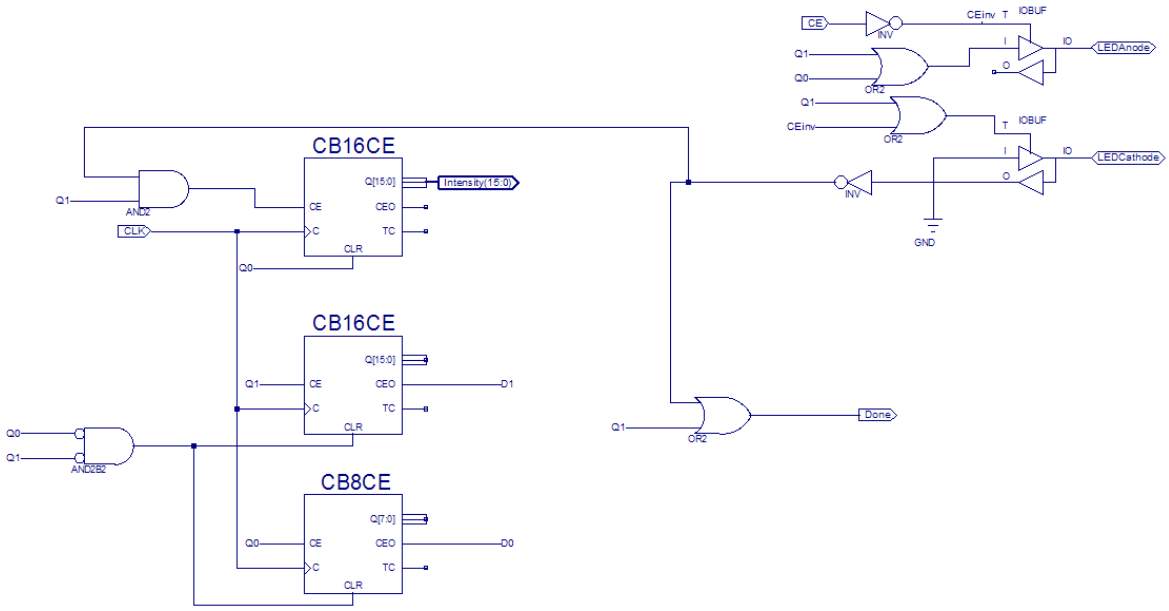

Figure 36: LED Sensor Schematic

The above sensing circuit is called by the higher-level Sensing_System block. The Sensing_System block has two states in it; LED baseline acquisition and unknown LED acquisition and adjustment. In the first state, button 0 is pressed until a satisfactory intensity is measured on the baseline LED. Each time a measurement is made in this state, it is stored using a 16 input D flip-flop. When button 1 is pressed, the circuit enters the adjustment phase. A custom VHDL module compares the baseline value stored by the flip-flop with the new measurement. If the new LED is brighter than the baseline, the current is decreased until they match, and if the new LED is dimmer the current is increased. During this state the 7-segment displays are alternating between displaying the most recent intensity measurement and the new current value.

2.7. Printed Circuit Board

Once our current driver and FPGA were functional, we started designing our Printed Circuit Board (PCB). Before we began the PCB layout, we made several changes to the rest of the

circuit. The first change we made was the addition of the power supply components. In our previous circuits, we just specified general voltage supplies. Our power supply design can be seen in Figure 37. We are using the LM340T voltage regulator, which can accept our input value of 15V and output 5V. The larger 100µF capacitors are used as storage capacitors, and the two other capacitors were specified by the datasheet. Looking at our power connector J1, we have connections for a 15V power supply and a second 15V connection for the FPGA. The diode is just added for protection, so that if we connect the power supply backwards, the current will flow through the diode instead of destroying any components of our circuit.

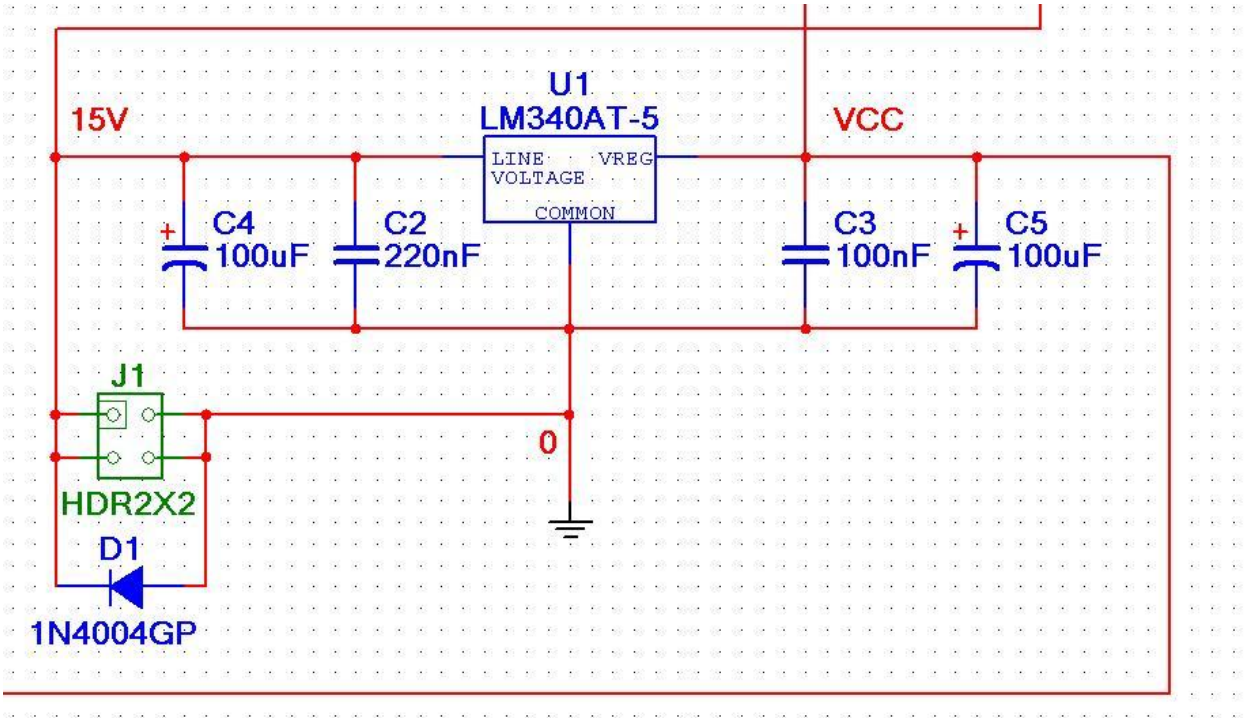

Figure 37: Power Supply Schematic

Next, we look at the changes made to the current source, which can be seen in Figure 38. The major change to this block was a change in feedback resistor values. In our original circuit, we had planned for a 2.5V input from the FPGA to correspond to a 250mA current in the LED. Since then, we have decided to utilize the full 3.3V range of the FPGA to determine the current value. This has forced us to change the value of the feedback resistors to obtain a gain around 12.9V/V. Additionally, we have included one right angled header that will connect the PCB to the DAC from the FPGA, and we have replaced the amplifier DIP package with a 8 pin DIP

socket, so that if we were to destroy the op-amp, we could just remove and replace the component, and still maintain a functional PCB.

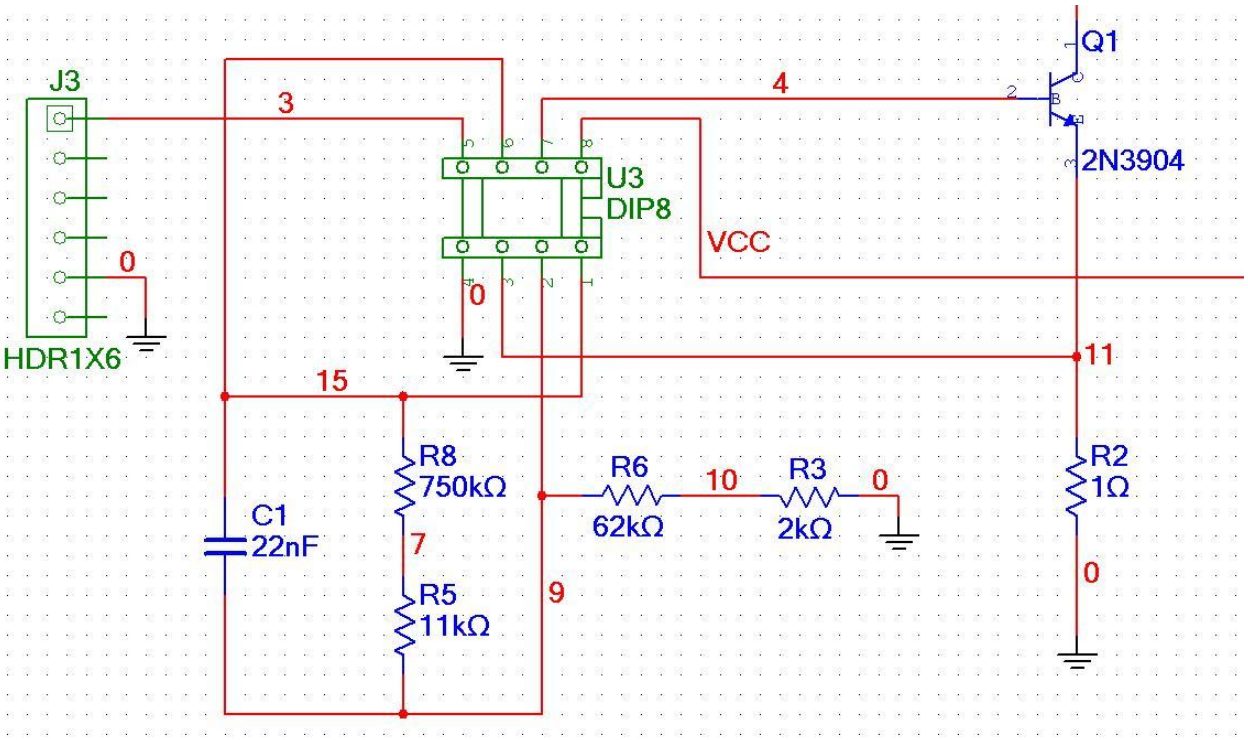

Figure 38: Updated Current Source

Finally, we made major changes to the MOSFET driver, which can be seen in Figure 39. While the MOSFET driver remains the same, modifications were made to the sequencing circuit. Since we wanted to drive two LEDs with this MOSFET driver, we placed each LED between two MOSFETs, which were connected in parallel between the power supply rail and the current source BJT. Nodes 21 and 18 were connected together so that the n-channel MOSFETs (BS170) and the p-channel MOSFETs (IRFD9210) would sink the current in an alternating fashion. A 2x2 header was added to replace the two LEDs so we could swap them easier. Header J2 connects the PCB to the FPGA so the PWM output can drive transistor Q5, and also connects to the anode and cathode of both LEDs, so the FPGA can sense the current in each LED. Resistors 4, 7, 9 and 10 were added to ensure that the FPGA would not see the 5V rail, as the absolute maximum for the FPGA inputs is 4.3V.

After updating the schematic, we could start the PCB layout design. Several checks and updates later, we had a completed PCB design. The top and bottom of the PCB can be seen in Figure 40.

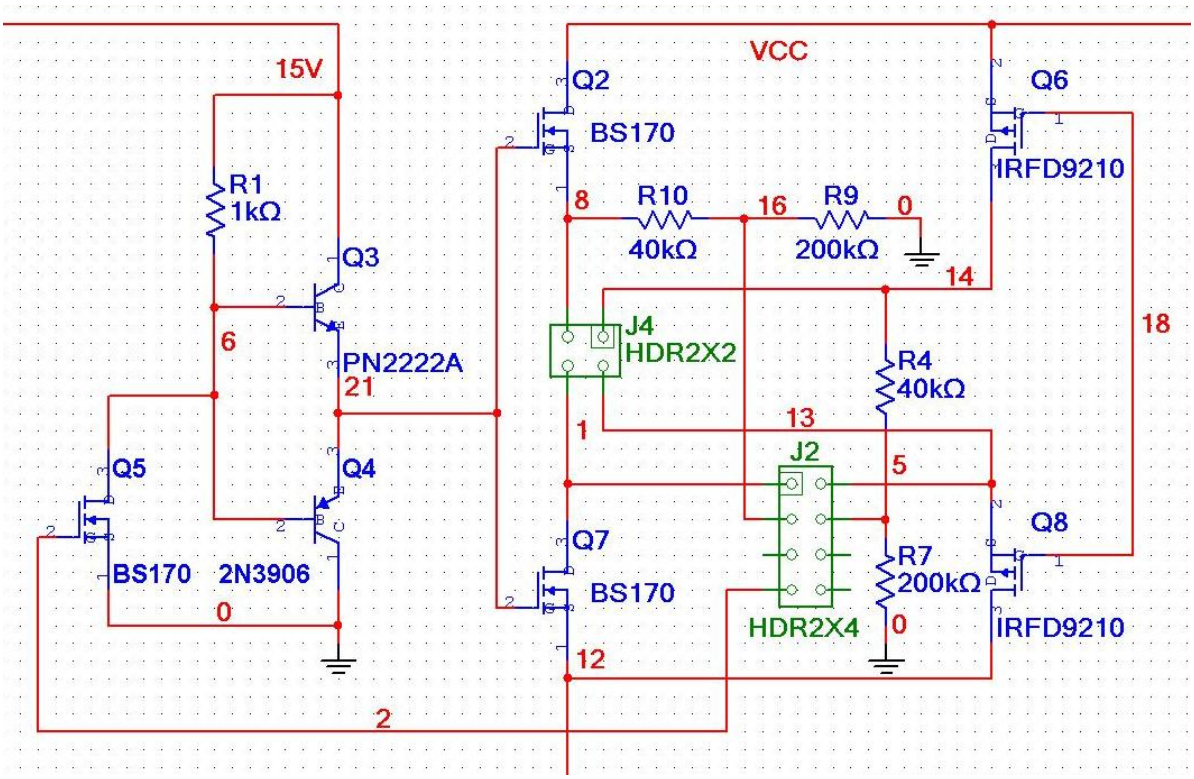

Figure 39: Updated MOSFET Driver

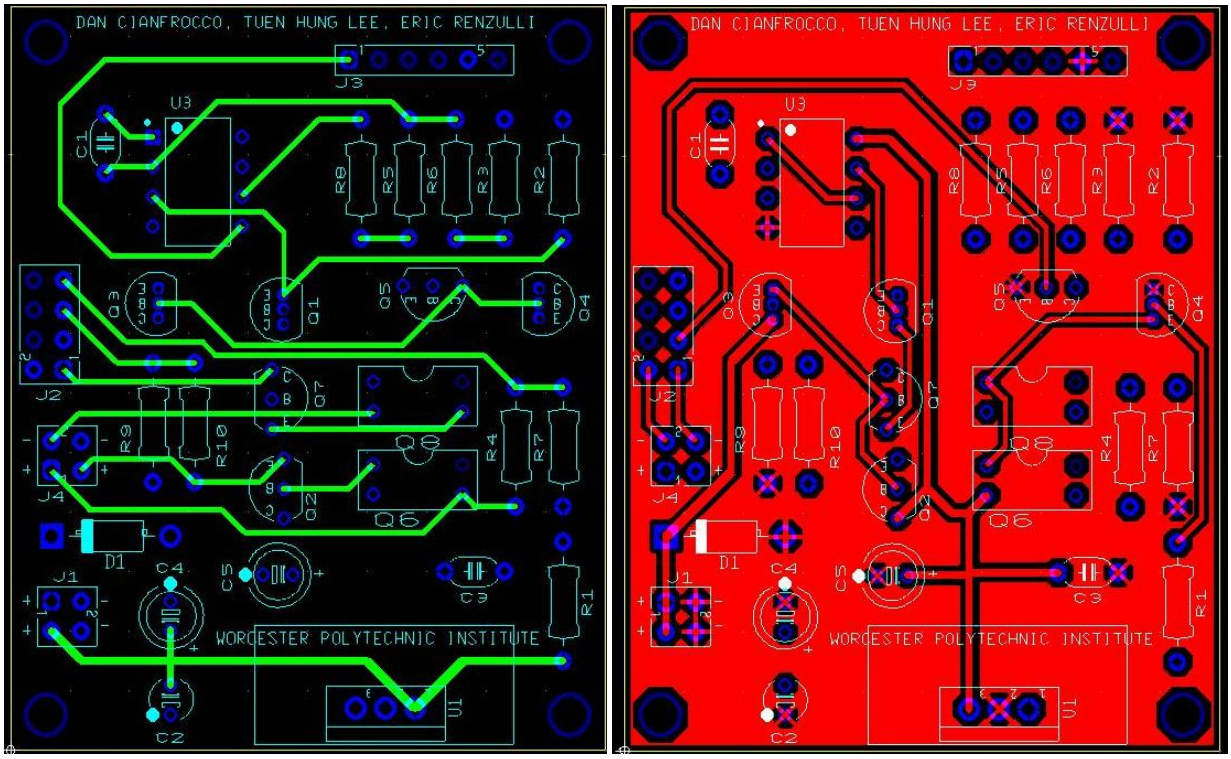

Figure 40: PCB Top (Green) and Bottom (Red)

About a week later, we received the PCBs. An unpopulated PCB can be seen in Figure 41.

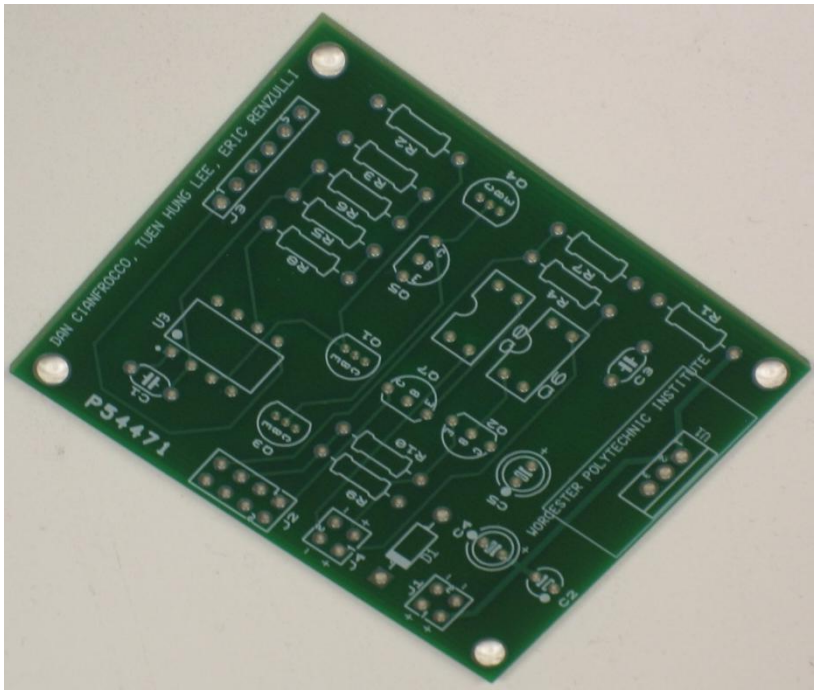

Figure 41: Unpopulated PCB

After receiving the PCB and soldering all the components, we experienced several problems during our initial testing. The first problem was with the resistor ratios between R10 and R9 as well as between R7 and R4. Our initial design limited the voltage on the FPGA to the absolute maximum rating. However, we decided to limit this voltage to the digital logic 'high' level of 3.3V, instead of the 4.3V maximum rating. We chose 1MΩ resistors for R9 and R7 and 510kΩ resistors for R10 and R4 to obtain the new desired ratio.

The next problem was that the BJT transistor footprints on the PCB were wrong. The individual pins were connected to the correct nodes, but the outline was backwards. While the B, C and E indicators on the PCB were correct, we followed the shape on the PCB when soldering these transistors instead of checking the pin layout on the datasheet. As a result, the transistors were in backwards. An annoying and easily avoided problem, since all we had to do was rotate transistors Q1, Q3 and Q4. Luckily, the base terminal was the center pin, so we did not damage any of the transistors.

The final problem was that the LED on the PMOS side of the MOSFET driver was not functioning properly. After probing several nodes on the PCB and observing the corresponding waveforms, we discovered that node 13 wasn't pulling the voltage low enough. After a simple MOSFET operating mode calculation, we determined that Q8 was operating in the saturation region. However, we want this transistor to act as a switch, so it needs to operate in the triode region. After closer inspection, we decided to replace this MOSFET with a BJT as the base to emitter drop is relative low compared to the gate to source voltage of the MOSFET. We chose a 2N3906 PNP transistor, and added a base resistance of 1kΩ to provide enough current to drive a maximum load of 250mA.

After these changes were made, the final populated PCB can be seen in Figure 42.

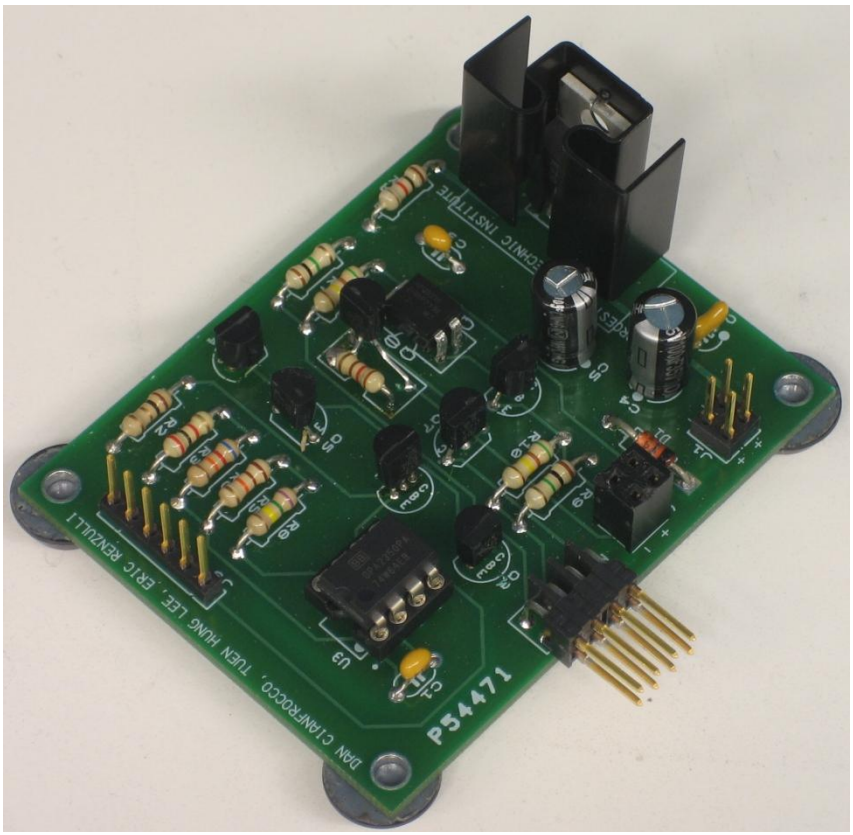

Figure 42: Final Populated PCB

3. Results and Analysis

After successfully completing a prototype, we tested the LEDs and observed how the overall circuit, software included, functioned as a whole. First, we used a spectrometer to analyze new and degraded LEDs to determine if there was any color shift caused by the lifetime testing or changes in the duty cycle of the driven LED. Next, we verified that our overall circuit was functional by testing the software and hardware together, making sure that each piece worked correctly.

3.1. LED Characterization

To perform our LED characterization, we visited the WPI IPG Photonics Laboratory, led by Professor Quimby. The instrument we used during our testing was the USB650 Red Tide Spectrometer (USB650 Red Tide Spectrometer for Education), manufactured by Ocean Optics, which can be seen in Figure 43. This spectrometer comes in a small package, as seen by the relative size of the USB connector, and was extended to our testing setup using a fiber optic cable. The spectrometer also came with software that made it very easy to record data, so all we had to do was swap the LEDs and then save the new data. We used our prototype to drive the LEDs, as seen from our test setup in Figure 44.

Figure 43: Red Tide Spectrometer

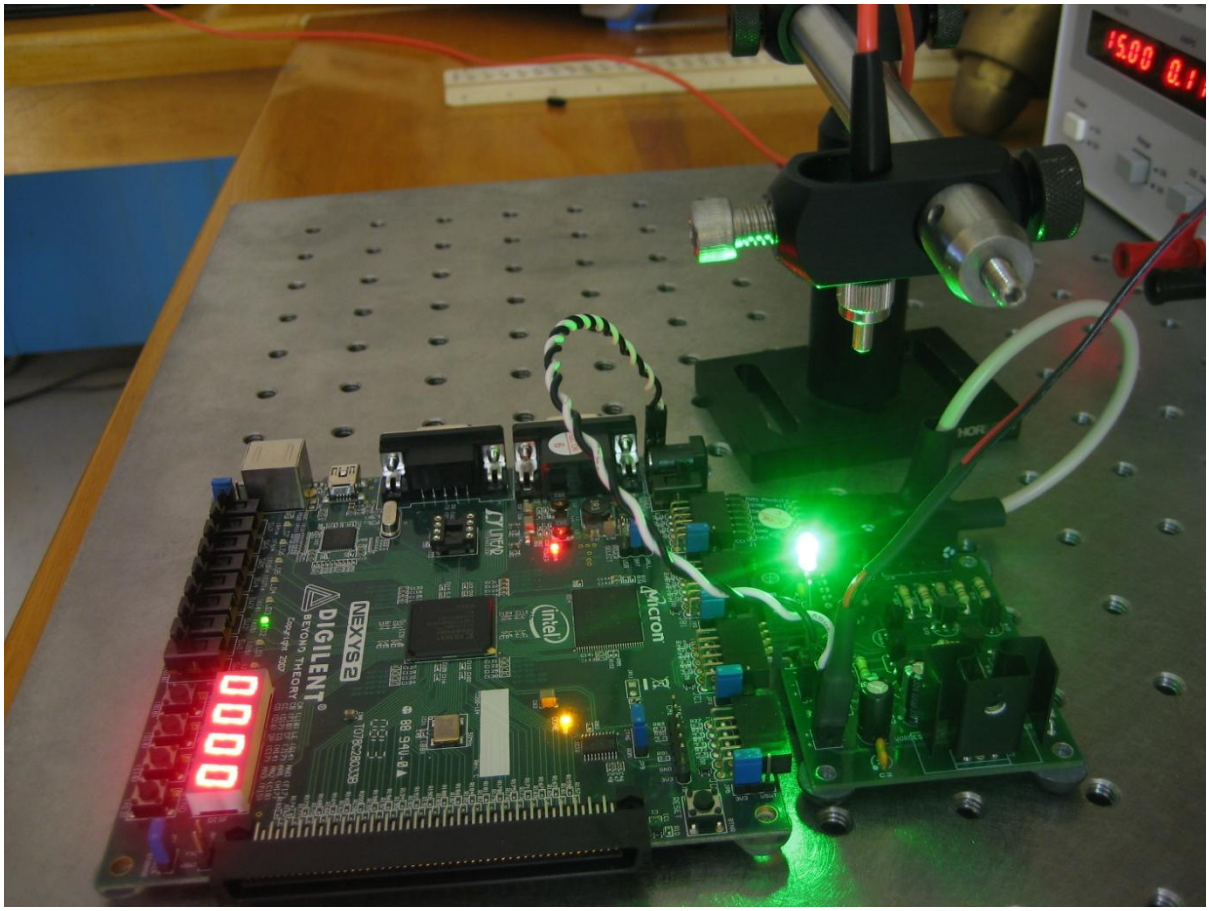

Figure 44: LED Characterization Test Setup

During our testing, we measured the emission spectrum of 2 new LEDs of each color from the same manufacturer and 2 degraded LEDs of each color from the same manufacturer. The new and degraded LEDs were driven with a DC current of 20mA. Additionally, we measured the emission spectrum of 2 LEDs per color manufactured by Avago being driven by a current of 100mA at 10% duty cycle.

The spectrum of the all the red Avago LEDs we tested can be seen in Figure 45. Comparing the three sets of data pairs, we can clearly see that there was not any significant spectrum shift between the new, degraded and PWM driven LEDs. They all reached a peak intensity between 630nm and 633nm.

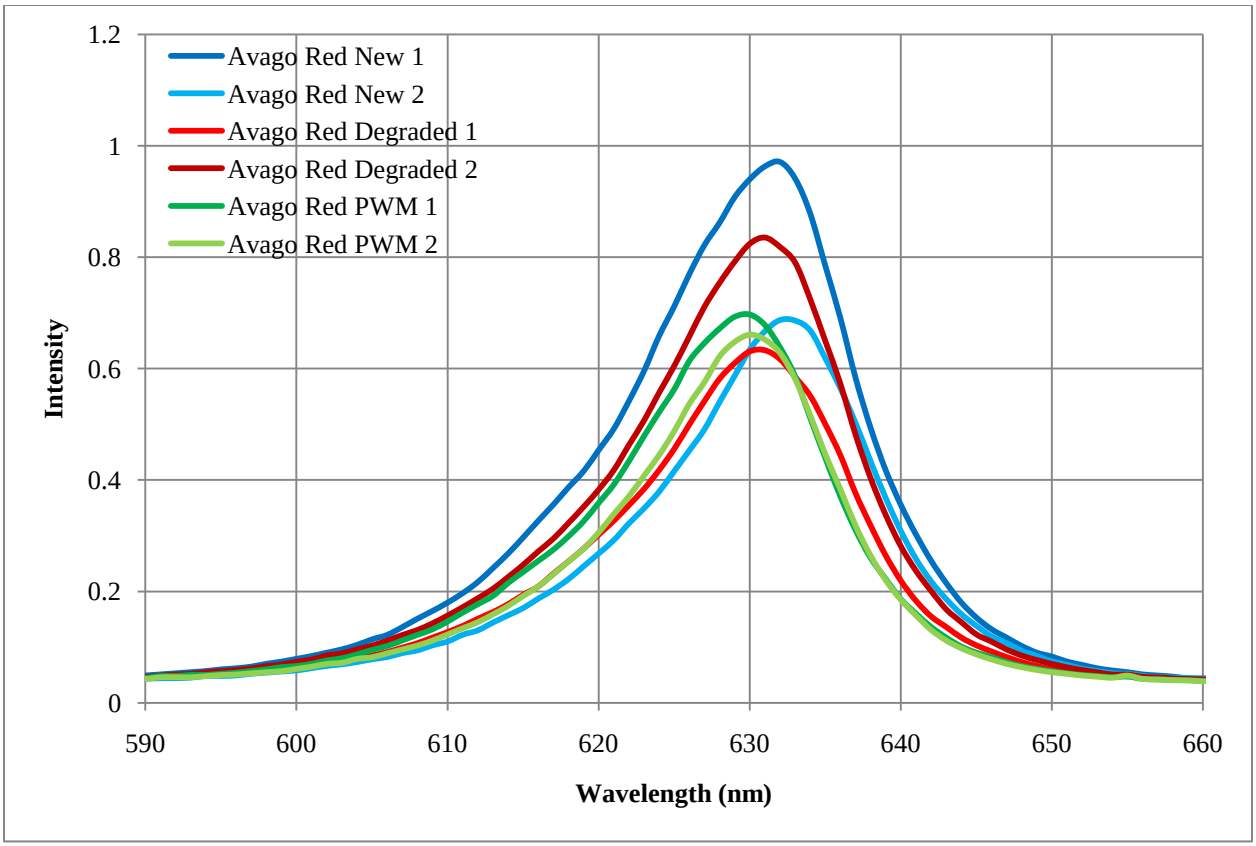

Figure 45: Avago Red LED Spectrometer Data

Looking at the other colors and manufacturers, we noticed the same pattern, that the peak wavelengths would fall within 3nm of each other. Given that this error could originate from the spectrometer measurements or the LED manufacturing process, we believe that these differences in the peak intensity wavelength are insignificant. Therefore, we will not be accounting for any color shift in our final prototype, just changes in intensity. All of our LED characterization results can be seen in the appendices.

3.2. Final Prototype

In order to verify our design we needed to test the two primary components separately. The first component we tested was the LED sensing software. For the test, we simply inserted an LED into the PMOD pin sockets and illuminated it with an LED of the same color. We started with the intensity counter running at 10kHz, but found that the intensity would saturate to '0' because the capacitance was discharging in less than 100µs. We found that a clock rate of 32kHz was

good for distant LEDs or LEDs reflecting off of a surface. When two LEDs were pointed head-to-head, however, we found that it was still saturating. We settled on a clock rate of 44kHz for our final implementation, which gives us a peak intensity around 10-20 clock cycles.

Next we verified the assembled PWM driving circuit. We began by subjectively observing the LEDs with varying drive frequency. We observed that both LEDs maintained the same brightness even with the PWM frequency set to 250kHz, which meant that our circuit was meeting expectations. We also observed a linear change in brightness as PWM was adjusted. These results were then verified using an oscilloscope in the figures shown below. Since the circuit is supposed to float both the anode and cathode during "off" time, you should expect the voltage to remain constant. However, Figure 46 shows a pronounced parasitic discharge of the floating nodes, and the parasitics of Figure 47 settle much faster.

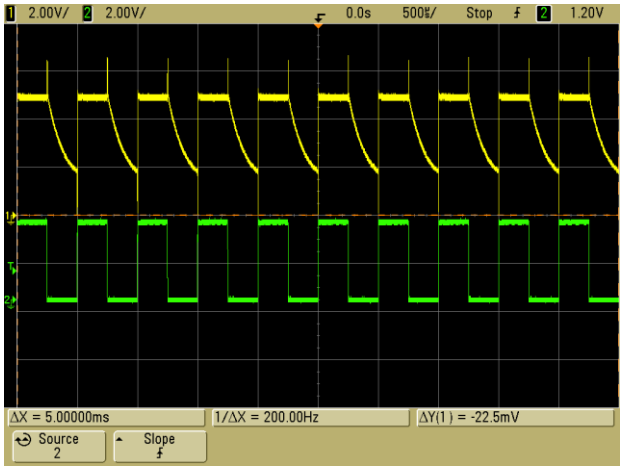

Figure 46: LED Cathode (Top) at 2kHz, (Bottom=PWM)

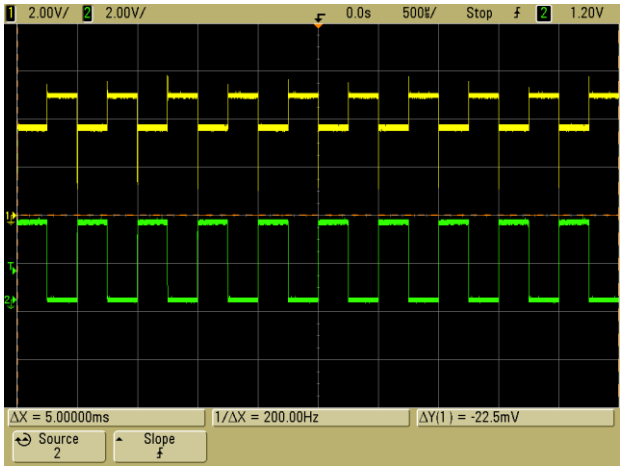

Figure 47: LED Anode (Top) at 2kHz, (Bottom=PWM)

With each component functioning properly, we could proceed with testing the complete circuit. Even with the extra voltage dividers and MOSFETs, our circuit was still successful at measuring a relative light intensity created by the PWM controller. For our demonstration, we configured our software to change the current when applying corrections to intensity. It successfully captured results, compared them, and then adjusted the current appropriately. As the samples are acquired, the current eventually settled on a new value that matched the desired output. We chose to change current so that we could generate a directly measurable result, however it is less

than ideal for real-world applications. As an LED decays, its output falls; to counteract this, either the current or the pulse-width need to change. If we increase the current, we are only going to accelerate the degradation, so changing the pulse-width is ideal. But in order to do this a mathematical relationship needs to be derived from a change in intensity to a change in pulse-width, and deriving the physical eye's integration of light was beyond the scope of our project.

A picture of our final prototype, including the FPGA, can be seen in Figure 48.

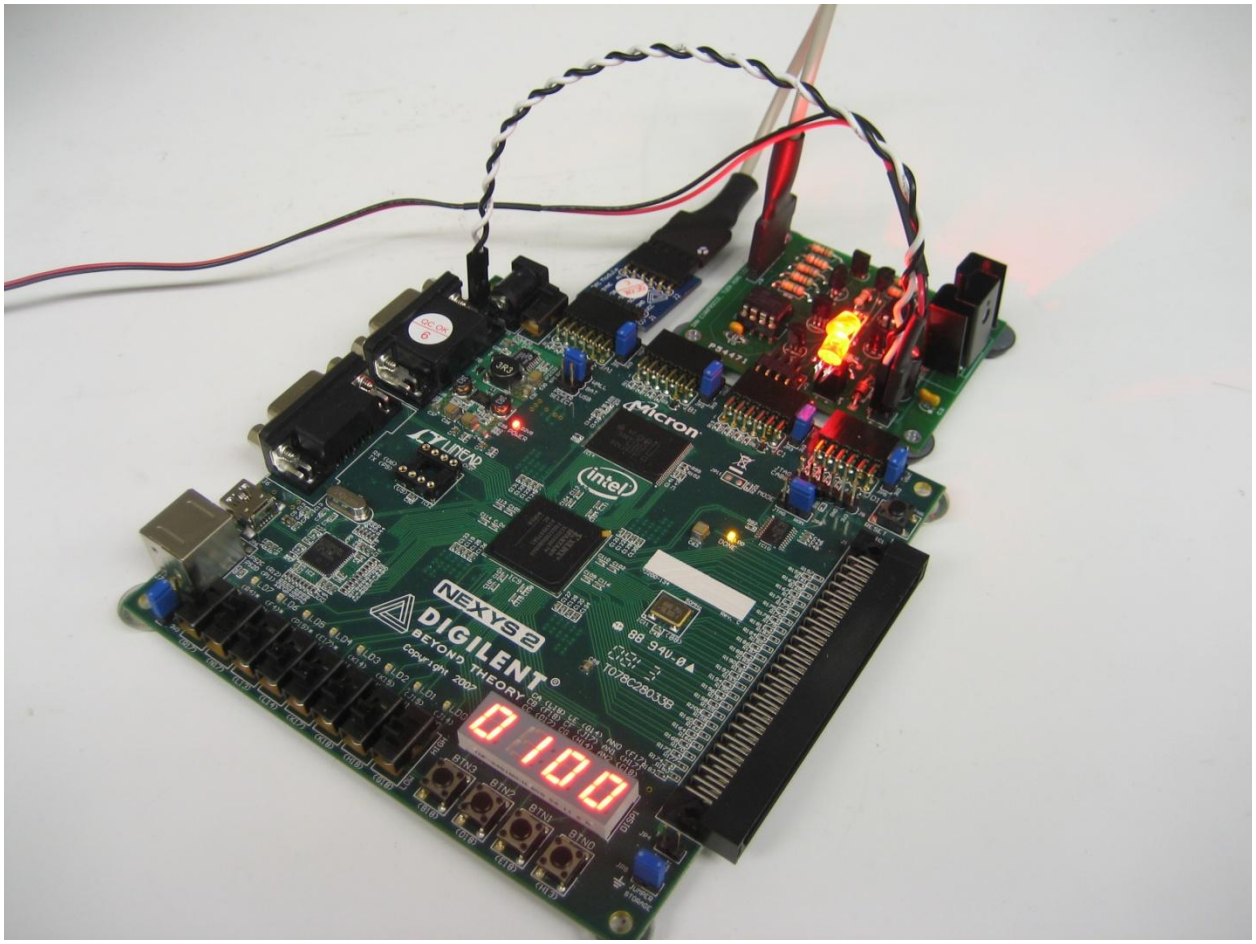

Figure 48: Final Prototype

4. Conclusion and Recommendations

The test system prototype demonstrated enough support that LEDs could be used as an emitter and as an optical feedback mechanism. The LEDs in the test system were able to emit light at desired current, frequency, and duty cycle. Additionally, in sense mode, the LEDs were effective in measuring the brightness of another LED of the same color. Using the data provided by the sensing LED, the feedback control system accurately adjusts the brightness to the desired level. Also, through degrading and characterizing the LEDs, we concluded the sensing ability of LEDs are not greatly impacted by degradation.

Though the project was a success, there are a few things we would like to improve. One of these improvements is to create better symmetry in the MOSFET driver. In the current design, NMOS transistors are used on one side and PMOS transistors are used on the other. Although this design requires only one gate driver, it creates asymmetry between the two sides due to different properties of the MOSFETs. A correction of this problem would be to use NMOS transistors on both sides of the driver. This way, the circuit would perform better, with a small increase in the component count. Another issue we would have liked to address is the LED degradation process. Due to the limited timeframe of this project, we degraded the LEDs in batches. LEDs of the same colors were degraded at the same time, while we monitored the degradation progress of only one of the LEDs in the batch. The assumption that all of the LEDs degraded the same way is very inaccurate, especially with different manufacturers. If we had more time, we would have degraded the LEDs in a more accurate fashion, either individually or in batches by color and manufacturer. Lastly, our design needs some work in optimizations. On the digital circuitry side, we are currently using about 60% of the gates available after optimizations from Xilinx. Considering the gates count on the FPGA board and the functionality of our digital circuit, the gate usage is high. One of the reasons for this was the floating point calculations, which we concluded were unnecessary in the late stage of the project. Replacing floating point modules with fixed point modules would greatly reduce the gate usage. On the analog circuitry side, capacitor C5 was found to be unnecessary on the output of the voltage regulator. Also, there were noise issues presented in the circuit originated by the PMOD digital to analog converter. While we could not make changes on the DAC, inserting a filtering capacitor would be enough to eliminate the noise.

If another group were to further expand on this project, we would recommend that they implement this technique on a larger scale. A large LED display is typically made up of smaller panels of LEDs. A system that drives and calibrates a panel of LEDs would be an ideal step forward. The challenges in this setup would be in modifying the existing power supply to support the increased number of LEDs. Additionally, the LED driving scheme would need to be changed due to the LED placement in columns and rows. The biggest challenge would be to devise an efficient and accurate LED sensing method that would satisfy every LED in the panel. Lastly, with information on all the LEDs, a control system that can interpret the data and calibrate the LEDs would not be easy to create. However, if all of these improvements were made, this technique would be ready to introduce into the LED display market.

The technique of using LEDs as an emitter and a sensor has potential. Our prototype has demonstrated this concept effectively. However, further research and development would be necessary before LEDs could be implemented as sensors in real world applications. We hope that this project is helpful for future advancements in video display applications.

5. Bibliography

Camarota, R. (2009, October). *Using LEDs as LIght-Level Sensors and Emmitters "LED Sensor and Emitter" Reference Design.* Retrieved March 7, 2010, from Altera: http://www.altera.com/literature/wp/wp-01076-led-driver-reduces-power-adjusting-intensity-ambient-light.pdf

Daktronics. (n.d.). *Permanent Installation Video Products*. Retrieved October 2, 2009, from http://www.daktronics.com/ProductsServices/Products/Video/Permanent/Pages/default.aspx

Dorsch, J. (2009). Daktronics, Inc. *Daktronics, Inc.*

Hamamatsu Photonics, K. K. (2008). *Photodiode Technical Guide*. Retrieved October 6, 2009, from http://sales.hamamatsu.com/assets/html/ssd/si-photodiode/index.htm

Harris, S. (2009). *Color and Luminance Uniformity Correction for LED Video Screens*. Retrieved October 14, 2009, from http://www.signindustry.com/led/articles/2007-10-15-SH-PulseWidthModulationPWMCorrectionOfLEDDisplays.php3#story

Harris, T. (2002, January 31). *How Light Emitting Diodes Work*. Retrieved October 19, 2009, from http://electronics.howstuffworks.com/led1.htm

Lee, M., Hillman, C., & Kim, D. (2005). *Industry News: How to predict failure mechanisms in LED and laser diodes*. Retrieved October 14, 2009, from http://mae.pennnet.com/Articles/Article_Display.cfm?ARTICLE_ID=230223&p=32&cat=Depar

Lighthouse Technologies Ltd. (2009, January 13). *R16i/o-II SPECIFICATIONS.* Retrieved from Lighthouse Technologies: http://www.lighthouse-tech.com/UserControl/Attachment/DownloadAttachment.ashx?photoid=1186895d-c5d0-4212-8553-d3a5f94679b6&size=Original&down=down

Maxim. (2003, Feb 25). *APPLICATION NOTE 1883*. Retrieved 10 18, 2009, from http://www.maxim-ic.com/appnotes.cfm/appnote_number/1883

Miyazaki, E., Itami, S., & Araki, T. (1998). Using a light-emitting diode as a high-speed, wavelength selective photodetector. *Review of Scientific Instruments , 69*, 3751-3754.

Nexys2 FPGA Board. (2008, June 21). Retrieved 12 19, 2009, from Digilent, Inc.: http://www.digilentinc.com/Data/Products/NEXYS2/Nexys2_rm.pdf

Shen, H., Pan, J., & Feng, H. (2006). Accelerated life test for high-power white LED based on spectroradiometric measurement. *Proceedings of SPIE, the International Society for Optical Engineering* .

The LED Light. (2000). *LED Technical Specifications and Application Notes*. Retrieved 10 18, 2009, from The LED Light: http://www.theledlight.com/technical1.html

Trevisanello, L., Meneghini, M., Mura, G., Vanzi, M., Pavesi, M., Meneghesso, G., et al. (2008, June). Accelerated Life Test of High Brightness Light Emitting Diodes. *IEEE TRANSACTIONS ON DEVICE AND MATERIALS RELIABILITY , 8* (2).

U.S. Department of Energy. (2008, September). ENERGY STAR Manufacturer's Guide for Qualifying Solid-State Lighting Luminaires.

USB650 Red Tide Spectrometer for Education. (n.d.). Retrieved March 3, 2010, from Ocean Optics: http://www.oceanoptics.com/Products/usb650.asp

Appendix A: Degraded LED Spectrometer Data

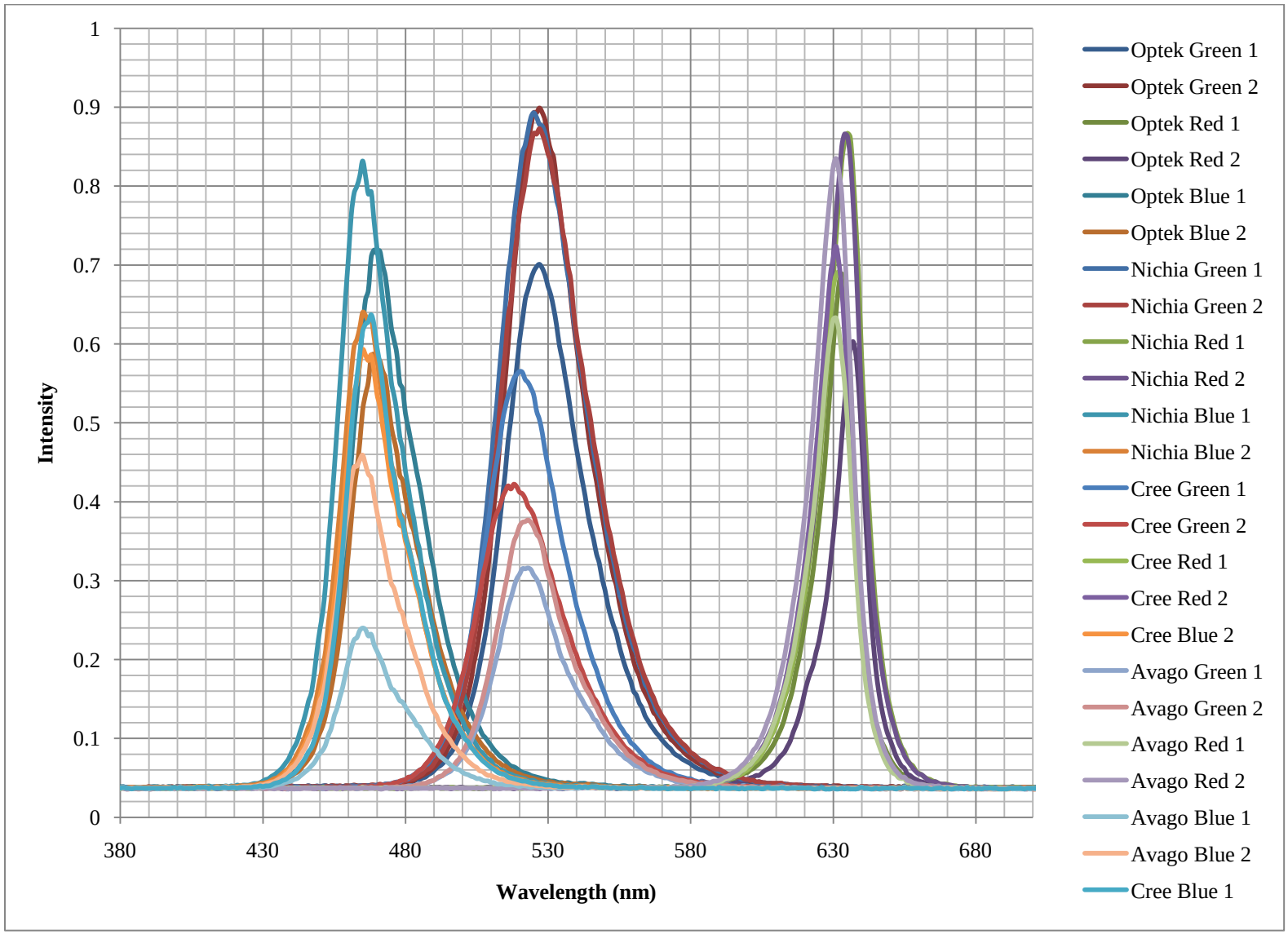

Appendix B: New LED Spectrometer Data

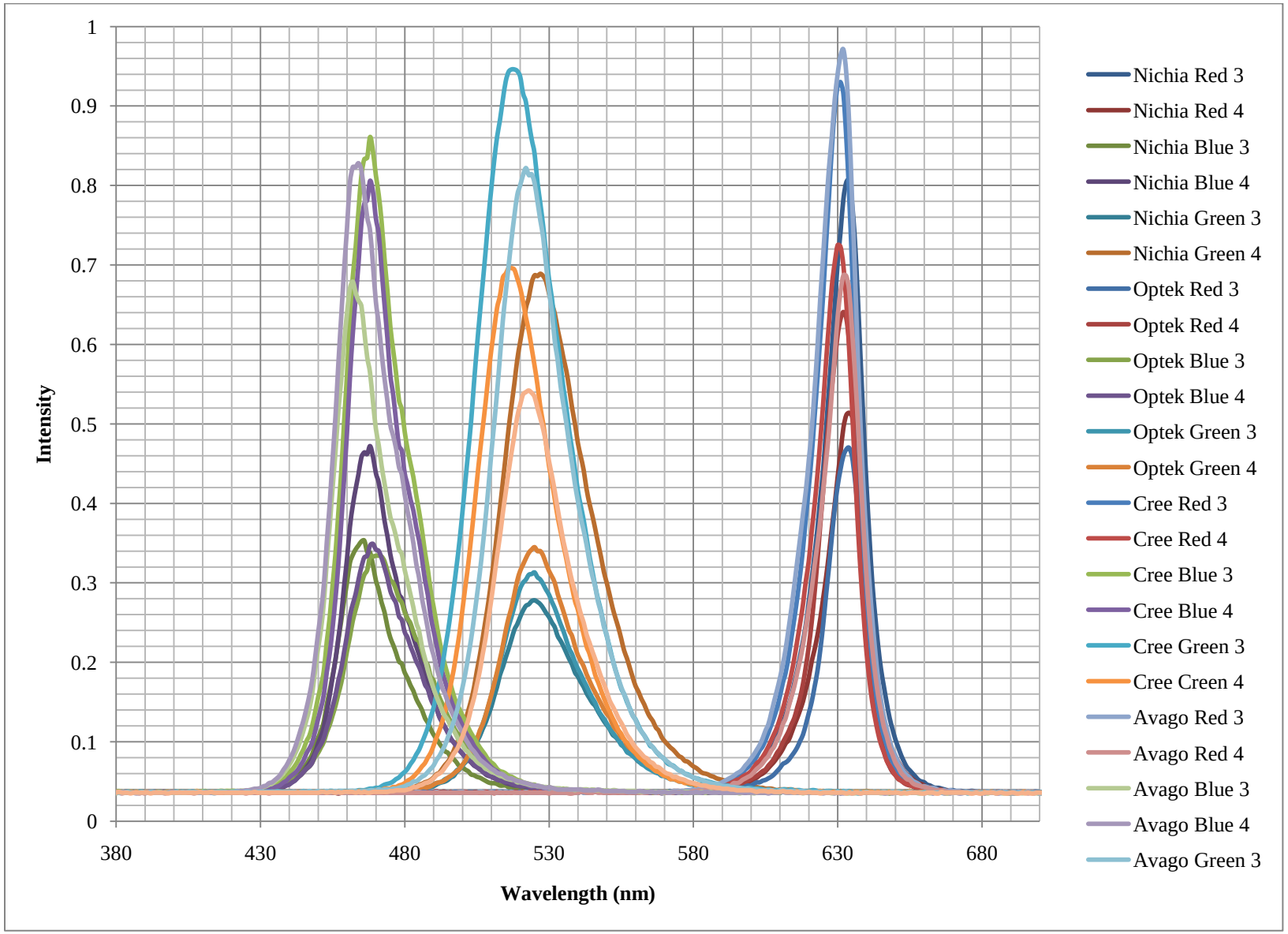

Appendix C: PWM Driven Avago LED Spectrometer Data

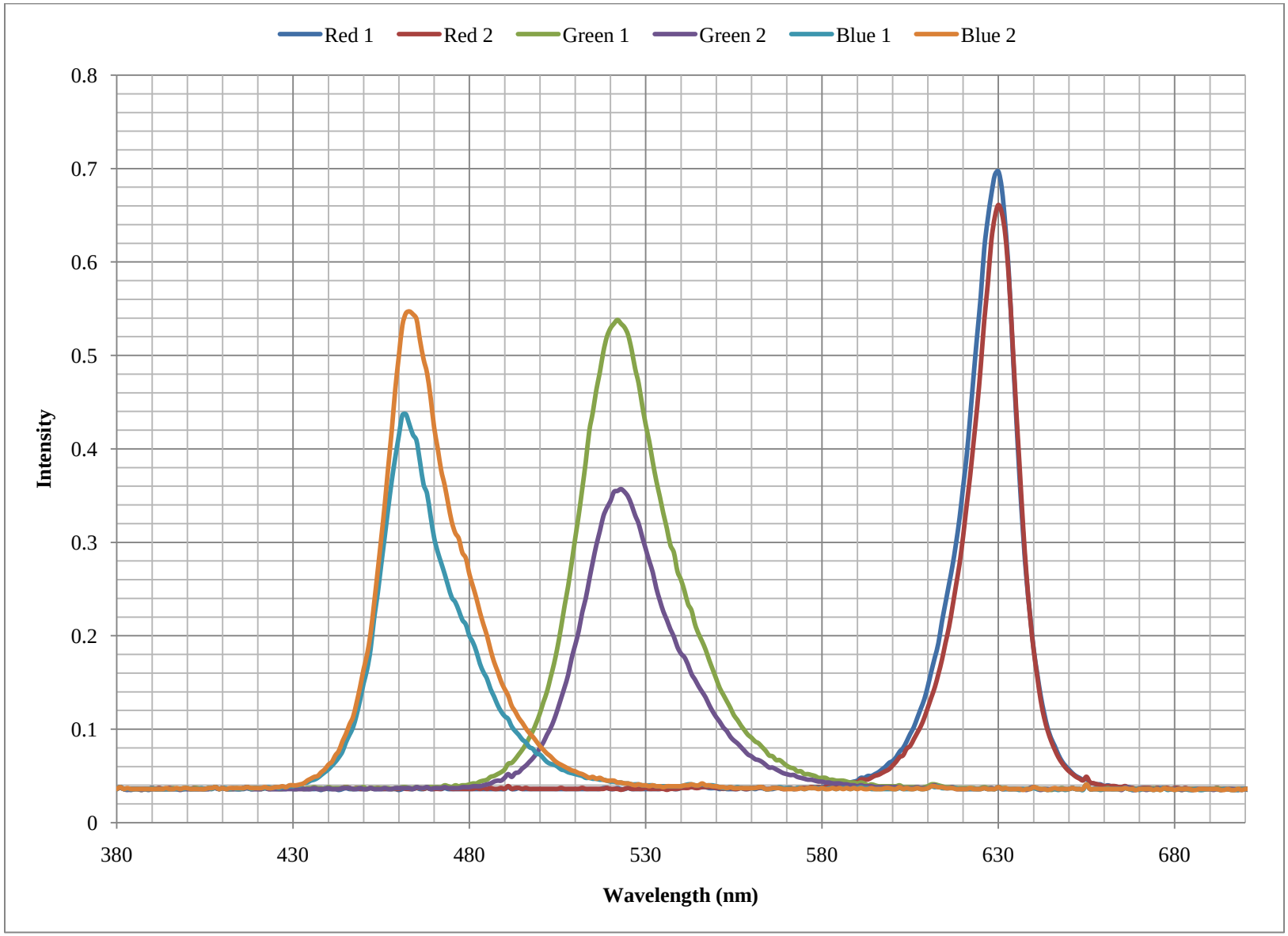

Appendix D: Parts Orders

Description	Distributor	Dist. Part No.	MFG	MFG Part No.	Unit	QTY	Sub
Voltage Regulator	Digikey	LM340T-5.0-ND	National Semiconductor	LM340T-5.0/NOPB	$ 1.74	2	$ 3.48
Dual Op-Amp	Digikey	OPA2350PA-ND	TI	OPA2350PA	$ 3.31	5	$ 16.55
JFET OP-AMP	Mouser	595-TL081BCP	TI	TL081BCP	$ 0.75	5	$ 3.75
100K Potentiometer	Mouser	594-64W104	Vishay/Sfernice	M64W104KB40	$ 1.44	2	$ 2.88
Switching Mosfet	Mouser	863-BS170RLRAG	ON-Semi	BS-170	$ 0.29	5	$ 1.45
Mosfet Driver	Mouser	863-MC34151PG	ON-Semi	MC34151	$ 0.99	3	$ 2.97
						Total:	$ 31.08
Dual Op-Amp	Mouser	595-OPA2350PA	TI	OPA2350PA	$ 3.30	5	$ 16.50
PMOS	Mouser	844-IRFD9210PBF	Vishay	IRFD9210PBF	$ 0.71	5	$ 3.55
Red LED	Mouser	828-OVLJRGD8	Optek	OVLJRGD8	$ 0.19	10	$ 1.90
Green LED	Mouser	828-OVLJGGD8	Optek	OVLJGGD8	$ 0.64	10	$ 6.40
Blue LED	Mouser	828-OVLJBGD8	Optek	OVLJBGD8	$ 0.47	10	$ 4.70
100uF Capacitor	Mouser	647-UHE2A101MPD	Nichicon	UHE2A101MPD	$ 0.29	10	$ 2.90
0.22uF Capacitor	Mouser	581-SR205E224MAR	AVX	SR205E224MAR	$ 0.19	5	$ 0.95
						Total	$ 36.90
Four 8-bit D/A PMOD	Digilent	Pmod-DA1	Digilent	Pmod-DA1	$19.99	1	$ 19.99
						Total	$ 19.99
CAP 100UF 35V ELECT NHG RADIAL	Digikey	P5551-ND	Panasonic - ECG	ECA-1VHG101	$ 0.14	10	$ 1.38
CONN HEADER FMAL 4PS .1" DL GOLD	Digikey	S7105-ND	Sullins Connector Solutions	PPPC022LFBN-RC	$ 0.55	2	$ 1.10
CONN HEADER VERT .100 6POS 15AU	Digikey	A26551-ND	Tyco Electronics	87224-6	$ 2.34	1	$ 2.34
CONN HEADER RT/A .100 8POS 15AU	Digikey	A26595-ND	Tyco Electronics	87230-4	$ 1.92	2	$ 3.84
CONN HEADER VERT .100 4POS 15AU	Digikey	A26567-ND	Tyco Electronics	87227-2	$ 1.77	1	$ 1.77
Voltage Regulator	Newark	41K4773	National Semiconductor	LM340T-5.0/NOPB	$ 1.77	2	$ 3.54
BS170 - MOSFET Transistor	Newark	58K8772	Fairchild Semconductor	BS170	$ 0.23	5	$ 1.15
HEATSINK TO-220 VERT MNT .75"	Digikey	HS198-ND	Aavid Thermalloy	574502B00000G	$ 0.40	2	$ 0.80
Jumper Wire - Female to Female Connector	Sparkfun	PRT-08614	Sparkfun	PRT-08614	$ 1.50	2	$ 3.00
						Total	$ 18.92

Appendix E: Letter to LED Manufacturers

Dear XXXXXXX,

We are three students currently pursuing a degree in Electrical and Computer Engineering at Worcester Polytechnic Institute in Worcester, Massachusetts. As part of our degree requirements, we must complete a Senior Project. For our project, we have decided to use three LEDs that XXXXXXX manufactures, with part numbers XXXXXX, XXXXX and XXXXXX. We have looked through many distributors and discovered that these LEDs are either not carried or are only sold in bulk. For our project, we only need ten of each LED. Is there any way that free samples could be provided or that only 10 of each LED can be purchased? If these specific LEDs can't be provided, please let us know the part numbers of similar LEDs that can be provided. A more detailed description of our project is as follows.

This project, called the Major Qualifying Project, represents the capstone of our education at Worcester Polytechnic Institute, as it tests our knowledge of Electrical and Computer Engineering as we must solve a complex problem similar to one we might encounter in our careers.

Our project is sponsored by The New England Center for Analog and Mixed Signal Integrated Circuit Design, a laboratory at WPI that is run by Professor John McNeill. The members of this lab include Allegro Microsystems, Analog Devices, BAE Systems, Texas Instruments and The National Science Foundation. These members provide funding and project opportunities for both undergraduate and graduate students.

Our project involves "Green" technologies and applications of Pulse Width Modulation. We chose to develop a proof-of-concept to show that Light Emitting Diodes can be used as light detectors. The first phase of our project is to characterize the spectrum and intensity of the LEDs we have selected. In the second phase of our project, we will develop feedback circuitry to automatically correct the intensity of an LED by observing the current through another LED biased to operate as a sensor.

The main goal of our project is to implement this system for video display applications, as most displays in use today do not have any auto-corrective features to adjust the intensity or color of the image. For our project, we have decided to use red, green and blue oval LEDs since many manufacturers use oval LEDs for outdoor video displays due to their wide viewing angles. We indexed LEDs from many different manufacturers and came up with a list that fit our criteria. We would like to use the three LEDs mentioned above for our project. Please let us know if this can be arranged.

We look forward to hearing from you.

Sincerely,
Dan Cianfrocco, Tuen Hung Lee, Eric Renzulli
The New England Center for Analog and Mixed Signal Integrated Circuit Design
Worcester Polytechnic Institute
Worcester, MA

Appendix F: Letter to Daktronics

Hello Mr. Dunkel,

As you may recall, we spoke at the beginning of September about my senior undergraduate capstone project at Worcester Polytechnic Institute. We are now reaching the end of the research phase of our project, and I was wondering if you would be willing to put me in touch with an engineer to answer several questions?

First some more information about our project: Our project is characterizing and applying Light Emitting Diodes as an optical feedback mechanism for large-scale video applications. We are beginning by running a variety of leaded LEDs designed for display applications through a series of tests to determine what the best traits are for LED sensing including emission and absorption spectrums, peak measured photocurrent, and the effect of higher peak currents during pulse-width-modulation. We then plan to implement a proof-of-concept control loop to calibrate LEDs for variations.

In order to provide the most useful proof-of-concept, there is some information we would like to know.

1. In what way do you drive your LEDs?
    a. Do you use PWM? If so, what frequency are you using? What is the maximum duty cycle?
    b. Do you drive the panels by sequencing through the rows and columns individually, or do you drive everything in parallel?
    c. How often is each entire panel refreshed?
2. Are you willing to share the manufacturer and part number of the typical LEDs you use?

By understanding the length of time each LED is driven, and how much dead time can be used for sensing, your information will be used to constrain our proof-of-concept to real-world scenarios. Additionally, providing the type of LEDs that you use will allow us to provide the most useful research data.

Thank you for your time, and I hope to hear from you soon.

Dan Cianfrocco, Tuen Hung Lee, Eric Renzulli
The New England Center for Mixed Signal and Analog Circuit Design
Worcester Polytechnic Institute
Worcester, MA

Appendix G: Datasheets